Muscle Organization in *Caenorhabditis elegans*: Localization of Proteins Implicated in Thin Filament Attachment and I-Band Organization

G. ROSS FRANCIS and ROBERT H. WATERSTON
Department of Genetics, Washington University School of Medicine, St. Louis, Missouri 63110

ABSTRACT The body wall muscle cells of *Caenorhabitis elegans* contain an obliquely striated myofibrillar lattice that is associated with the cell membrane through two structures: an M-line analogue in the A-band and a Z-disc analogue, or dense-body, in the I-band. By using a fraction enriched in these structures as an immunogen for hybridoma production, we prepared monoclonal antibodies that identify four components of the I-band as determined by immunofluorescence and Western transfer analysis. A major constituent of the dense-body is a 107,000-D polypeptide that shares determinants with vertebrate α-actinin. A second dense-body constituent is a more basic and antigenically distinct 107,000-D polypeptide that is localized to a narrow domain of the dense-body at or subjacent to the plasma membrane. This basic dense-body polypeptide is also found at certain cell boundaries where thin filaments in half-bands terminate at membrane-associated structures termed attachment plaques. A third, unidentified antigen is also found closely apposed to the cell membrane in regions of not only the dense-body and attachment plaque, but also the M-line analogue. Finally, a fourth high molecular weight antigen, composed of two polypeptides of ~400,000-D, is localized to the I-band regions surrounding the dense-body. The attachment of the dense-body to the cell surface and the differential localization of the dense-body–associated antigens suggest a model for their organization in which the unidentified antigen is a cell surface component, and the two 107,000-D polypeptides define different cytoplasmic domains of the dense-body.

Comparative studies of muscle structure have revealed many distinct muscle types in invertebrates where specialized requirements for contraction appear to be met by modifications of a common design. One such type, found in nematodes and in some other invertebrates, is an obliquely striated musculature whose structure has been described as intermediate between classical striated and smooth muscle types (43, 44). As typified in the body wall muscle of nematodes such as *Ascaris* (43) and *Caenorhabditis elegans* (33, 60), the distinctive feature of sarcomere organization in this muscle type is that the A-I striations run obliquely to the axes of myofilaments rather than at a 90° angle as in cross-striated muscle. In place of Z-discs, thin filaments attach to dense-body structures and, as in smooth muscle, there are prominent connections between contractile elements and the cell surface at intervals along the entire length of the cell rather than principally at opposite ends of the cell (26, 43).

Our interest in *C. elegans* muscle has arisen as part of investigations of the genetic specification of muscle development and structure in this animal. More than 20 genes that can mutate to affect the normal lattice structure of the *C. elegans* body wall musculature have already been identified, and the products of several genes have been determined (12, 36, 59–61, 68). The most intensively studied gene, *unc-54*, encodes the principal myosin heavy chain isoform of the body wall muscles (34, 36), and evidence indicates that another, *unc-15*, specifies the thick filament core protein, paramyosin (59). In addition, mutations in each of three clustered actin genes (14) have been recovered (29, 61), and the product of one other gene, *unc-22*, has been identified as a myofibrillar component (Barstead, R., L. Schrieffer, D. G. Moerman, and R. H. Waterston, unpublished observations). With a knowl-

edge of their encoded products, these genes and their mutant alleles have proved useful in detailed molecular–genetic studies of myofilament assembly and function (35, 38–40).

In searching for the products of other genes affecting muscle structure, it is reasonable to consider not only additional components of the thin and thick filaments, but also accessory components necessary for the assembly and continued stability of the myofilament lattice. Many accessory proteins have been isolated from vertebrate skeletal muscle, studied by physiochemical methods, and localized in the sarcomere using antibodies raised against them. Some components, represented by the Z-line protein α-actinin (22) and several M-line proteins (54, 55), are thought to be constituents of specific substructures that interconnect thin or thick filaments, whereas the distributions of others are less readily interpreted in terms of their possible functions in muscle structure and contraction (11, 57, 58). The opportunity for genetic analysis of related proteins in *C. elegans* encouraged us to undertake experiments to identify additional proteins of nematode muscle as an initial step toward the characterization of mutations altering particular proteins. In seeking to identify components of the dense-body and other accessory structures of the body wall muscle, we produced hybridomas against a fraction enriched for these structures and screened their supernatants by immunofluorescence microscopy for monoclonal antibodies that revealed particular structures in the body wall musculature. In this paper, we describe the use of monoclonal antibodies for characterization of a high molecular weight I-band component and two distinct 107,000-D polypeptides of the dense-body that are positioned differentially within it. In addition, evidence that the dense-body and an M-line analogue are attached to the muscle cell surface is presented, and the localization of an unidentified antigen to regions near their sites of membrane attachment is described. The implications of these results for muscle structure and assembly are discussed.

MATERIALS AND METHODS

Nematode Strains and Culture: The Bristol strain of *C. elegans* was cultured and grown in gram quantities using methods reported previously (6, 47). All experiments used the wild-type strain N2, with the exception that strain RW89, which is homozygous for the *sup-12X* allele, *st89*, was also examined by electron microscopy. *sup-12(st89)* suppresses mutants alleles of the muscle affecting gene *unc-60* (60); by itself *sup-12(st89)* has no obvious effect on myofilament organization in animals that are otherwise wild-type (Francis, G. R., and R. H. Waterston, unpublished observations).

Preparation of Nematode Proteins for Immunizations and Antigen Characterization: Total nematode protein lysates were prepared by suspending 1 ml (packed volume) of worms in 4 ml of hot (100°C) 8 M guanidine-HCl in lysis buffer (50 mM Tris-HCl, pH 8.0, 2 mM EDTA, 1 mM phenylmethylsulfonyl fluoride [PMSF],[1] 100 U/ml Trasylol, and 10 μg/ml each of leupeptin, chymostatin, and pepstatin [all protease inhibitors from Sigma Chemical Co, St. Louis, MO]), and then alkylating solubilized proteins with iodoacetamide (62). The extract was dialyzed against 8 M urea in lysis buffer for 5 h, and then overnight against SDS gel sample buffer (32).

Protein fractions enriched in nematode muscle components were prepared by the procedures outlined in Fig. 1. 1 vol refers throughout to 1 ml of solution per 1 g initial wet weight of nematodes, and, except where noted, all steps were done at 0–4°C. Nematodes suspended in 10 vol buffer A (7.5 mM Na₂PO₄, pH 7.0, 40 mM NaCl, 1 mM EDTA, 1 mM PMSF) were passed twice through a
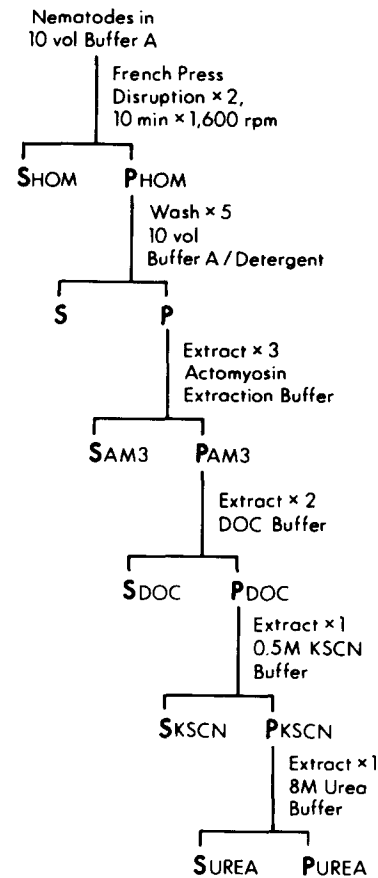
FIGURE 1 Outline of the procedures used for fractionation of nematode components. 1 vol refers throughout to 1 ml of solution per 1 g initial wet wt nematodes. *S*, supernatant; *P*, pellet; *buffer A/detergent*, buffer A/1% NP-40/0.02% deoxycholate.

40 ml French pressure cell adjusted to 3,500–4,000 psi, and the resulting homogenate was centrifuged (10 min, 1,600 rpm). The pellet was washed by five successive low-speed sedimentations (10 min, 1,600 rpm) in 10 vol of buffer A/1% Nonidet P-40 (NP-40)/0.02% deoxycholate, and then once in buffer A without detergent. The washed pellet was extracted by sequential 10-min incubations in (a) 1 vol actomyosin extraction buffer (50 mM Na₂HPO₄, pH 7.6, 0.6 M NaCl, 1 mM EGTA, 2 mM MgCl₂, 1 mM PMSF, 5 mM ATP), three times; (b) ⅓ vol DOC buffer (10 mM imidazole, pH 7.0, 0.4% deoxycholate, 1 mM EDTA, 1 mM PMSF), twice at 20–23°C; (c) ⅓ vol KSCN buffer (50 mM Tris-HCl, pH 8.0, 0.5 M KSCN, 50 mM Na₂SO₃, 1 mM EDTA, 1 mM PMSF, 5 mM ATP), once; and (d) ¼ vol 8 M urea in 20 mM Tris-HCl, pH 8.0, 1 mM EDTA, 1 mM PMSF, at 20–23°C. The particulate fraction was collected by centrifugation (10 min, 10,000 rpm) after each extraction.

Two 107,000-D (107-kD) polypeptides were prepared as a mixture from KSCN buffer extracts prepared as outlined in Fig. 1, with the modifications that the treatment with DOC buffer was omitted and the extraction in 0.5 M KSCN buffer was performed twice. The combined KSCN supernatants (15 ml) were made 40% saturated in (NH₄)₂SO₄ by the addition of a saturated solution at 0°C and the resulting precipitate was collected by centrifugation (10 min, 10,000 rpm), resuspended in 3 ml of 10 mM Na₂HPO₄, pH 7.4, 0.6 M NaCl, 2 mM dithiothreitol, 10 mM NaN₃, and applied to a Sepharose-4B column (1.5 × 80 cm) pre-equilibrated in the same buffer. Pooled 3-ml fractions containing the 107-kD polypeptides, which eluted reproducibly after the peak paramyosin (Mᵣ 103,000) fractions, were dialyzed against 10 mM NH₄HCO₃, 0.1 mM EDTA, 0.5 mM PMSF, and lyophilized. The 107-kD polypeptides were further purified by elution from preparative acrylamide/SDS gels as described by MacLeod et al. (36). A New Zealand white rabbit was immunized subcutaneously with ~80 μg of eluted protein emulsified in Freund's complete adjuvant, and again 3 wk and 8 wk later with 200 μg and 50 μg, respectively, of antigen in Freund's incomplete adjuvant. Immune serum was collected 10 d after the last injection, and an IgG fraction prepared by precipitation with (NH₄)₂SO₄ (22).

The immunogen for monoclonal antibody production was prepared from the high-salt-extracted AM-3 pellet described in Fig. 1. The pellet was washed

once in 20 vol of phosphate-buffered saline (PBS; 8.1 mM Na_2HPO_4, 1.8 mM KH_2PO_4, 140 mM NaCl, 2.7 mM KCl, pH 7.3), and then dispersed in a minimal volume of PBS. A fraction of this slurry was mixed directly with adjuvant, while another part was made 0.4% in SDS, heated 5 min at 80°C, and centrifuged to remove SDS-insoluble components (10 min, 15,000 g). BALB/c mice were immunized with the following schedule: 0.2 ml native antigen in Freund's complete adjuvant given subcutaneously; 2 mo later with the same in Freund's incomplete adjuvant; and 3 mo later with 0.5 ml of SDS-soluble components in Freund's incomplete adjuvant given intraperitoneally (i.p.). Serum taken after the third injection was analyzed by immunofluorescence of nematodes, and one strongly responding mouse was given a final i.p. injection of 0.5 ml of SDS-soluble components 3 d before being killed for hybridoma fusion.

Extraction of Nematodes for Microscopy: For use in immunofluorescence experiments, nematodes in 40 vol of buffer A were sheared by passage through a 40 ml French pressure cell adjusted to 200-240 psi. This range generally sliced the majority of adults and L3 and L4 stage larvae transversely at 1-5 sites, generating fragments of worms with lengths ranging from short pieces to nearly full-length animals lacking only small portions of the anterior or posterior anatomy. The worm fragments and surviving unbroken animals were collected by centrifugation (5 min, 1,600 rpm), resuspended in 30% sucrose, and centrifuged to remove undisrupted worms by flotation (47). The pelleted fragments were washed by allowing them to settle at unit gravity through 2-3 changes (20-30 min each) of 40 vol buffer A/1% NP-40. After one further wash in buffer A, the fragments were fixed in 3% formaldehyde (prepared from paraformaldehyde [41]) or by dilution of formalin (Fisher Scientific Co., Pittsburgh, PA) in 0.1 M Na_2PO_4 (pH 7.2) for 15 min at 0°C. Alternate fixation conditions used in some experiments were −20°C methanol (5 min) or −20°C 95% ethanol/5% acetic acid (5 min). Fixed samples were washed three times in PBS.

For observation with polarizing optics, NP-40-washed worm fragments were extracted for 20 min at 0°C in 10 vol actomyosin extraction buffer, and then fixed in 3% formaldehyde. In preparation for electron microscopy, adult hermaphrodites were dissected into 4-5 equal length fragments by a series of transverse slices made with a fractured razor blade. The cut fragments were extracted in three changes of buffer A/1% NP-40 at 0°C over 30 min, and then in 10 μl of actomyosin extraction buffer for 1 h at 0°C. Samples were then fixed overnight in cold 3% glutaraldehyde in 0.1 M Na_2PO_4.

Hybridoma and Monoclonal Antibody Production: Hybridomas were produced by fusion of mouse spleen cells to the Sp2/0-Ag14 mouse myeloma cell line (46) according to the method of Galfre et al. (16). Cells were plated in six 96-well culture dishes (0.2 ml/well) and grown under established culture conditions (15). After 3 wk of growth, supernatants from nearly confluent wells (~90% of total) were screened by indirect immunofluorescence of NP-40-washed worm fragments (see below). First stage incubations contained 100 μl of supernatant and 25 μl of packed fragments pooled from samples fixed separately with formaldehyde, methanol, or acid-alcohol as described above. Fluorescein isothiocyanate (FITC)–conjugated goat anti-mouse IgG (Cappel Laboratories, Cochranville, PA) was diluted 80-fold in PBS for second stage incubations. Selected hybridoma lines were cloned in soft agar (15) using normal 3T3 cells as a feeder layer, and re-cloned without the use of feeder cells. The heavy chain subclass of each monoclonal antibody was determined by the immunodiffusion method of Blose et al. (4) using subclass specific rabbit anti-mouse IgG sera (Litton Bionetics, Kensington, MD). Monoclonal antibodies MH23, MH24, MH35, MH40, MH45, and MH47 were IgG_1, and MH25, MH29, and MH44 were IgG2a.

Cloned hybridoma cell lines were grown as ascites tumors in BALB/c mice (15), and monoclonal antibodies were partially purified from ascites fluid by precipitation with 45% saturated $(NH_4)_2SO_4$ (51). Monoclonal antibodies MH23, MH24, MH35, and MH40 were purified further by DEAE-Sephacel (Sigma Chemical Co) chromatography (51), and were then conjugated separately to FITC (Aldrich Chemical Co, Milwaukee, WI) and tetramethyl-rhodamine isothiocyanate (TMRITC; Research Organics Inc., Cleveland, OH) according to the dialysis method described by Goldman (19). Conjugates were separated from free fluorochrome on a Sephadex-G25 column (0.6 × 20 cm) equilibrated in PBS/0.02% NaN_3.

Immunocytochemistry Procedures: Observations of immunofluorescence staining were made most frequently with the French-press sheared, NP-40-washed nematode fragments. Antibody incubations were carried out by combining ~25 μl of gravity-settled fragments in a microfuge tube with 0.5-1.5 ml of antibody diluted in PBS/0.02% NaN_3/10% normal goat serum, and gently mixing the tubes on a rotary shaker for 6-12 h. For direct staining, MH23 and MH24, conjugated with FITC, and MH35 and MH40, conjugated with TMRITC, were used at 14-18 μg/ml. For indirect labeling with other monoclonal antibodies (MH25, MH29, MH39, MH44, MH45, and MH47, and in some experiments MH23 and MH24), $(NH_4)_2SO_4$-fractionated ascitic

antibody was diluted 200-fold. Secondary incubations were then carried out similarly in 0.2 ml PBS/0.02% NaN_3/10% normal goat serum containing 10–14 μg/ml of affinity-purified goat anti-mouse IgG (Jackson Immunoresearch Labs, Inc., Avondale, PA). After each incubation, the fragments were collected by brief centrifugation (1.5 min, setting 4 of a clinical centrifuge), and washed with three 10-min changes of 1.5 ml PBS/0.02% NaN_3. In some experiments with formaldehyde-fixed samples, the F-actin-binding phallotoxin, phalloidin (66), conjugated with fluorescein (Molecular Probes, Inc., Junction City, OR) was added to 0.055 μM to the mixtures for direct immunofluorescence or to the secondary incubations for indirect staining.

For comparison with NP-40-washed fragments, immunofluorescence experiments were also done with nematodes made permeable to antibody by (a) fixation and protease digestion and (b) squashing. In the former procedure, animals were fixed with 3% formaldehyde and extracted with acetone as described previously (61), except that the formaldehyde fixation was for 12 h at 20-23°C. Fixed samples were then combined with 50 vol of a solution containing either subtilisin (1-5 U/ml in 0.1 M Tris-HCl, pH 7.4; Type VII protease, Sigma Chemical Co), or elastase (10-30 U/ml, Sigma Type II in 0.1 M Tris-HCl, pH 8.8), and incubated at 37°C for 4-8 h with gentle agitation. The animals were washed repeatedly with PBS/1 mM EDTA and then processed for immunofluorescence as described above for fragmented worms. Under the conditions used, ~10% of adults and L3 and L4 larvae treated with either protease were stained uniformly by each antibody class; the remainder were stained in localized areas or not at all. Nematode squashes were prepared by transferring 2 μl of concentrated suspension of worms in M9 buffer (6) onto several sites of a glass slide that had been precoated with 0.2% bovine serum albumin (BSA), overlaying a second clean slide onto the first, and applying gentle finger pressure. The squashes were frozen on dry ice for 5 min, and after prying the slides apart, the coated slide was placed in methanol at −20°C for 5 min and then rinsed in PBS. Antibody incubations were carried out essentially as described by Gossett et al. (21) using ascites fluid diluted 400-fold and affinity-purified TMRITC-goat anti-mouse IgG at 11 μg/ml.

Rabbit muscle myofibrils were prepared as described by Knight and Trinick (27) from strips of psoas muscle that had been tied at rest length to wooden sticks and glycerinated 4 mo at −20°C. Coverslips with adhering myofibrils were overlaid with 100 μl of a 50-fold dilution of rabbit immune (or preimmune) serum to the 107,000 M_r polypeptides in PBS/1 mM EDTA/0.02% NaN_3/10% normal goat serum, incubated 30 min, and then rinsed for 30 min in three changes of PBS/EDTA/NaN_3. A second incubation with FITC-conjugated F(ab)$_2$ fragment of goat anti-rabbit IgG (Cappel Laboratories) diluted 50-fold was done similarly.

Epitope Analysis: The following qualitative immunofluorescence assay was used to determine whether the class 1 antibodies MH35 and MH40 and the class 2 antibodies MH23 and MH24 recognized the same or different epitopes on their respective antigens. NP-40-washed worm fragments (15 μl in 200 μl of PBS/0.02% NaN_3) were first incubated with excess unlabeled antibody (1/20 dilution of ascites fluid corresponding to 150-300 μg/ml of antibody) for 12 h. An FITC-antibody conjugate of either the same antibody or a different antibody to the same antigen was then added to 12-14 μl/ml, and the mixtures were left for an additional 2 h. After three rinses with PBS, the samples were examined by fluorescence microscopy for diminished fluorescence intensity in comparison with samples preincubated with an irrelevant monoclonal IgG to a different antigen. In the control experiments, fluorescence signals were diminished markedly in samples stained with each FITC-conjugate after preincubation with the corresponding unlabeled antibody.

Microscopy: A Zeiss Universal microscope (Carl Zeiss, Inc., Thornwood, NY) equipped with epifluorescent illumination and selective filters was used to view and record fluorescence from samples mounted in a 1:1 mixture of PBS/glycerol. Kodak Tri-X and Ilford HP-5 films were exposed 10-25 s and developed in Diafine (Acufine, Inc., Chicago, IL) to an exposure index of 1,200. Methods used for polarized-light microscopy and the processing of nematodes for electron microscopy were as described previously (40, 60). In the electron micrograph reconstruction analysis, transverse thin sections (gray to silver) were cut through the length of one overlapping pair of body wall muscle cells at a level just posterior to the pharynx; each muscle quadrant in every tenth section was photographed separately at a magnification of 6,100.

Acrylamide Gel Electrophoresis and Western Transfer Analysis: Protein fractions were separated by denaturing acrylamide gel electrophoresis essentially as described by Laemmli (32), or, for two-dimensional gel electrophoresis, with minor modifications of the method of O'Farrell (42). Separated proteins were visualized by staining with 0.05% Coomassie Brilliant Blue R-250 in 50% methanol/7% acetic acid and destaining in 20% methanol/7% acetic acid. Alternatively, proteins were transferred to 0.45-μm pore nitrocellulose (NC) filter paper (Schleicher & Schuell, Inc., Keene NH) by the electrophoretic method of Towbin et al. (52). Transfer was overnight at 100 mA in a Bio-Rad (Bio-Rad Laboratories, Richmond, Ca) apparatus containing

12.5 mM Tris, 96 mM glycine, 20% (vol/vol) methanol. After incubation in 0.1% Tween-20 in Tris-buffered saline (TBS; 10 mM Tris-HCl, pH 7.4, 0.9% NaCl) for 15 min to block excess binding sites (3), the filters were processed by sequential incubations in (a) monoclonal antibody (250- to 400-fold dilution of ascites fluid), 8–12 h; (b) 2.5 µg/ml affinity-purified rabbit anti–mouse IgG (Gateway Immunosera, Inc., St. Louis, MO), 2 h; and (c) 0.05 µCi/ml ¹²⁵I-protein A (Amersham Corp., Arlington Heights, IL), 2 h. Each incubation was in TBS/0.1% Tween-20 with gentle shaking, and was followed by four to six 10-min washes in 200 ml TBS/0.1% Tween-20. NC filters reacted with rabbit serum antibodies were processed similarly, but with a 400-fold dilution of serum and 0.05 µCi/ml ¹²⁵I-protein A. Processed filters were stained with amido black (0.001% in 50% methanol/7% acetic acid), and then exposed to Kodak XAR-5 film with a DuPont Cronex Lightning-plus AC screen (DuPont Co., Wilmington, DE) for 3–48 h at −70°C.

Affinity Purification of Serum Antibodies: The subset of anti-bodies in a rabbit serum raised to nematode 107-kD proteins that also bound to chicken α-actinin were affinity-purified by a procedure adapted from the strategy of Krohne et al. (28). 400 µg of purified chicken gizzard α-actinin, prepared according to Feramisco and Burridge (13), was electrophoresed on each of two 7.5% SDS-gels, and transferred to NC. The filters were immersed in 25% isopropanol/7% acetic acid for 2 min, and a narrow strip was then cut parallel to the direction of migration, stained with amido black, and used to guide the cutting of the α-actinin band from the unstained portions of the filters. Excised strips containing α-actinin were incubated 15 min in TBS/0.1% Tween-20, and then 12 h in 40 ml of a 100-fold dilution of serum antibodies to the nematode 107,000 M_r polypeptides (in TBS/0.01% Tween-20). The strips were then rinsed in five 10-min changes of TBS/0.1% Tween-20 and overlaid with 4 ml of 0.1 M glycine-HCl, pH 2.2, 50 mM KCl for 3 min to elute bound antibody. The eluate was adjusted to neutral pH by the addition of ¹⁄₂₀ vol 1 M Tris pH 8.0 and 0.1 M NaOH, and diluted 10-fold in TBS/0.1% Tween-20 for incubation with NC replicas of two-dimensional gels (16 ml/transfer).

RESULTS

Review of Nematode Body Wall Muscle Anatomy

C. elegans body wall muscle cells are divided among four longitudinal strips that extend down the length of the animal, subventrally and subdorsally. In the adult there are 95 muscle cells, with 23 cells in the left subventral quadrant and 24 cells in all others (48). The cells are rhomboid-shaped and arranged as interlocking pairs within each quadrant, forming a double longitudinal row (Fig. 2a). As described previously (33, 64, 69), all but the most anterior and posterior cells in the adult contain 9–10 A- and I- band pairs arranged in a single layer that extends no deeper than 1.5 µm from the broad cell surface adjacent to the cuticle and the intervening hypodermal cell layer (Fig. 2, b and c). The contractile filaments are arranged longitudinally, and in the radial direction adjacent filaments are in register (diagrammed in Figs. 2b and 3a). In the circumferential direction, however, adjacent filaments are staggered relative to one another, which accounts for the oblique A–I striations that traverse the cell at an angle of ~6° (35) with respect to the filament axes (and the long body-axis).

The obliquely striated organization of the body wall muscle allows one to view both thick and thin filaments and accessory structures at different levels in a single transverse-section electron micrograph (Fig. 3b). In A-bands, the most central two columns of thick filaments are sectioned near their bare zones and appear to be aligned about amorphous material that by analogy to cross-striated muscle appears to represent an M-line analogue (Fig. 3c). This M-line broadens slightly near the plasma membrane where it joins more densely staining material. In place of Z-discs, thin filaments attach to a discontinuous row of dense-bodies centered in each I-band. In transverse sections, the dense-bodies are seen as intensely staining, finger-like structures projecting from plasma membrane. A basement membrane lies between the muscle cells

and the hypodermis, and in some sections its morphology appears specialized in regions overlying dense-body and M-line by the presence of distinctive cell surface material not seen elsewhere (Fig. 3, c and d).

As can be seen in Fig. 2a, each cell adjoins two to four other muscle cells and also has a free boundary along one edge of the muscle quadrant, either medially or laterally. In reconstructing sarcomere organization from electron micrographs of semi-serial transverse sections, we found that the cell boundaries could be distinguished as being of two types that differed in their orientation and the structures associated with them. One type was found at the edges of the muscle quadrants and at muscle cell junctions that extended approximately parallel to the long body-axis. In these regions, filaments in alternating A- and I-bands were oriented parallel to the adjoining cell surface, and thin filaments appeared to end at the last dense-body in each I-band. The other type was found where cell boundaries were oriented obliquely and thus intersected the longitudinal arrays of contractile filaments. These cell margins were bordered by thin filaments which, when traced in semi-serial sections, were found to be organized in half I-bands; that is, filaments extended from the overlap zone of the A-band directly to the cell boundary. There, the filaments appeared to end in densely staining plaques on the inner surface of the cell membrane rather than at bipolar dense-bodies (Fig. 3b). We refer to these structures as attachment plaques to distinguish them from dense-bodies because, as is shown below, the two structures differ in composition as well as in appearance.

Extraction of Muscle Components for Monoclonal Antibody Production

The association of the dense body and M-line analogue with the cell membrane suggested that both structures may attach to it and possibly to the adjacent basement membrane. To evaluate this hypothesis, we examined muscle structure in permeabilized worms that had been extracted in a 1% NP-40 solution, and in some cases, with an actomyosin extraction buffer containing 0.6 M NaCl and ATP. Polarized-light microscopy of NP-40–washed fragments, generated by limited French-press shearing, revealed the same interspersion of A- and I-bands as found in living animals, with normal placement of birefringent dense-bodies in the I-band (Fig. 4, a and b). Subsequent treatment with actomyosin extraction buffer at 0–4°C led to a rapid loss of birefringence from A-bands, but had a lesser effect on dense-body birefringence during a 20-min incubation (Fig. 4c). To verify that the dense-bodies withstand high-salt extraction, hand-dissected animals were extracted with 1% NP-40 and 0.6 M NaCl, and then examined by electron microscopy (Fig. 3e). Thick and thin filaments were greatly reduced in number in the extracted fragments, but remaining elements, including the dense-bodies, stayed closely associated with the hypodermis and cuticle. Most of the residual thick filament mass was restricted to the center of A-bands and frequently appeared to be clustered about M-line material. Despite the apparent solubilization of the cell membrane, both the dense-body and the M-line substance appeared to be affixed to the basement membrane, implying that each structure may be joined to the basement membrane by insoluble trans-membrane components. In the hypodermis, filaments appeared to extend from the basement membrane to densely staining structures on the inner surface of
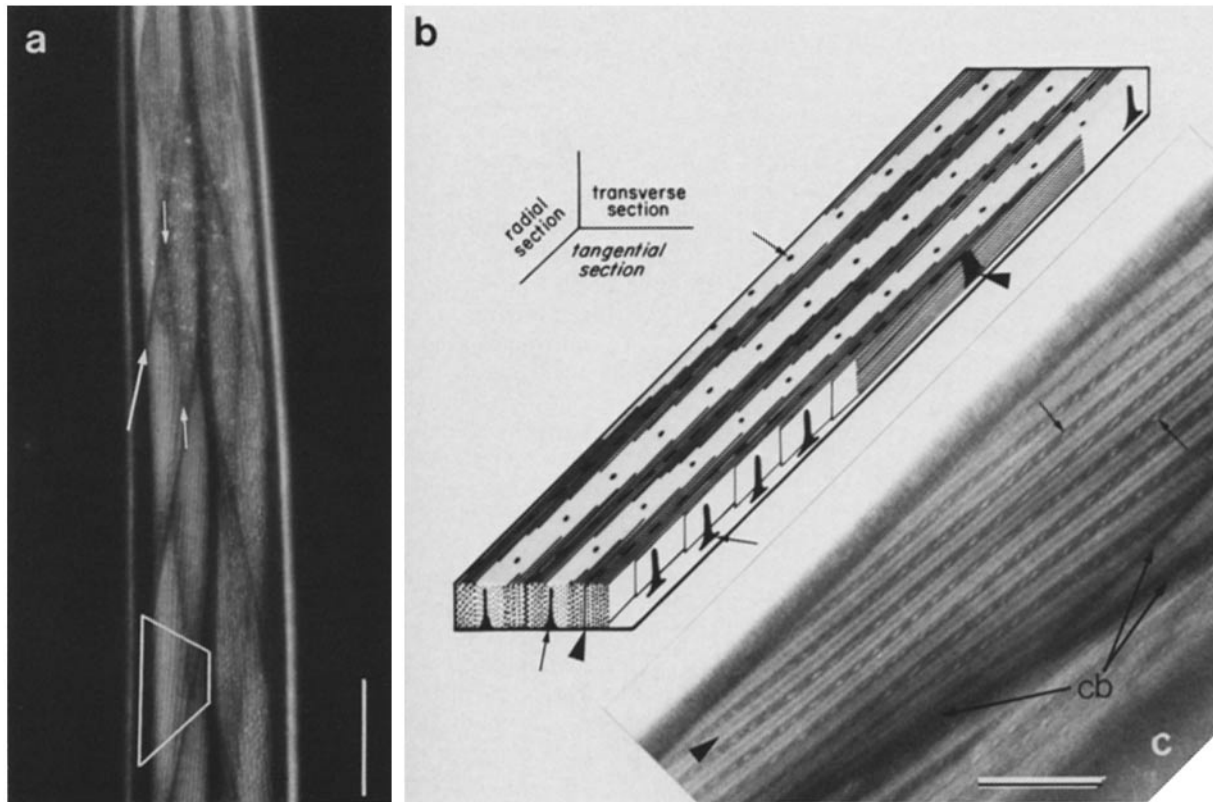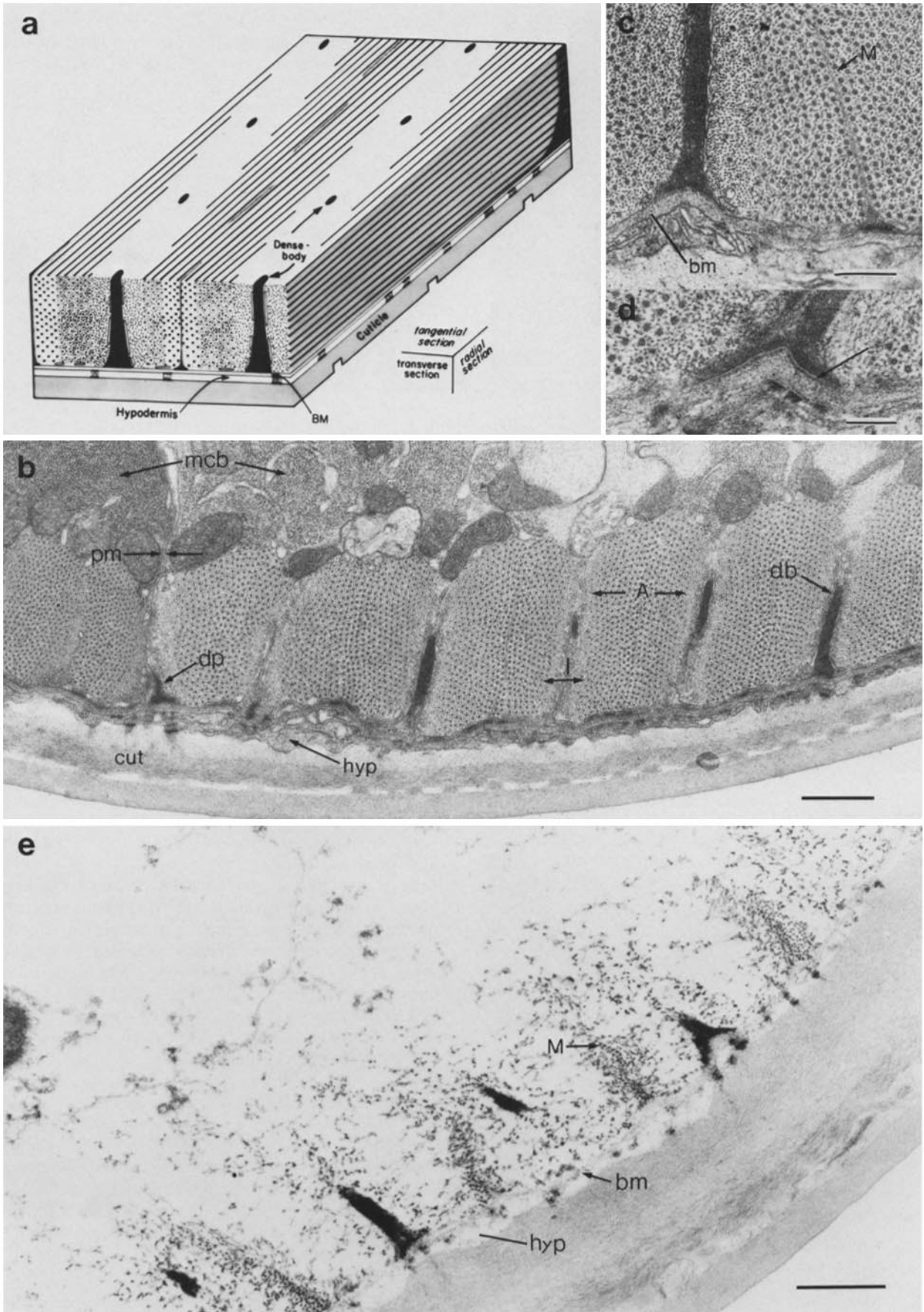
FIGURE 2   Body wall muscle organization. (a) Polarized-light micrograph of an anterior region of an adult showing muscle cell packing in each of two quadrants. The birefringent striations run obliquely to the long axis. Approximate cell boundaries (arrows) are present as areas of reduced birefringence. Large arrow, an oblique cell boundary where half-I-bands are found in electron micrographs; small arrows, a longitudinal cell boundary. A region corresponding to the boxed area is shown in c. Bar, 50 μm. $\times$ 310. (b) Diagram of the contractile lattice in three planes. The top surface (tangential section) illustrates the arrangement of A-(dark) and I-bands (light), and dense-bodies (arrows) as they appear when viewed with polarizing optics (but with reverse contrast, and the cell membrane at bottom). Thick filaments and the M-line analogue (arrowheads) are drawn, but thin filaments have been omitted except in transverse section. Adjacent thick filaments are in register in radial section (side) but are staggered in tangential section (staggering of adjacent thick filament columns is also shown by the cut-away at lower right). (c) High power ($\times$ 1,650) polarized-light micrograph with A-I striations oriented parallel to the those drawn in b. Birefringent A-bands, with a darker H-zone (arrowhead), alternate with dark I-bands, each containing a row of birefringent dense-bodies (arrows). cb, muscle–muscle cell boundaries. Bar, 10 μm.

the cuticle that resembled hemidesmosomes.

Acrylamide gel electrophoresis confirmed that the high-salt treatment solubilized a major fraction of the previously characterized nematode myofilament proteins: myosin, paramyosin, actin, and tropomyosin (24, 25) (see below, Fig. 11).

We reasoned that since components of the dense-body, M-line analogue, and other structural elements should be enriched for in the detergent, high-salt extracted fragments relative to known myofilament proteins, the preparation should serve as a useful immunogen for production of mono-

FIGURE 3   Body wall muscle ultrastructure. (a) Diagram illustrating myofilament organization in three planes of section for interpretation of electron micrographs. Thin filaments are omitted except in transverse section (front). (b) Electron micrograph of wild-type in transverse section. The contractile lattice lies adjacent to the cell surface that underlies the hypodermis (hyp) and cuticle; organelles lie more interiorly, in the muscle cell body (mcb). Myofilaments, seen in cross-section, are arranged in alternating A-(A) and I-(I) bands. Dense-bodies (db) project from the cell membrane that lies adjacent to the hypodermis (hyp) and cuticle (cut). Membrane vesicles, probably sarcoplasmic reticulum, are present along the surfaces of the dense-body. A half I-band attachment plaque (dp) is present on the inner surface of the plasmalemma (pm) at the junction of two cells. Bar, 0.5 μm. $\times$ 27,500. (c and d) Higher magnification micrographs showing the dense-body and the M-line (M) in wild-type (c) and in an animal homozygous for the mutation sup-12(st89). A basement membrane (bm) lies between the muscle cell and hypodermis, and distinctive extracellular material (arrow) is present where the cell surface underlies the dense-body and M-line. This material can be seen in wild-type, but for unknown reasons it has been most conspicuous in sections of animals homozygous the sup-12 allele st89. (Muscle ultrastructure of sup-12(st89) animals is difficult to distinguish from wild-type, but there may be subtle changes in filament organization [Francis, G., unpublished observations]). (c) Bar, 0.2 μm. $\times$ 57,000. (d) Bar, 0.25 μm. $\times$ 42,000. (e) Dissected worm extracted with 1% NP-40 and actomyosin extraction buffer. Residual thick filament material appears to be clustered around M-line material (M). Dense-bodies and the M-line material remain closely associated with the basement membrane (bm) and hypodermis (hyp). Bar, 0.5 μm. $\times$ 31,000.
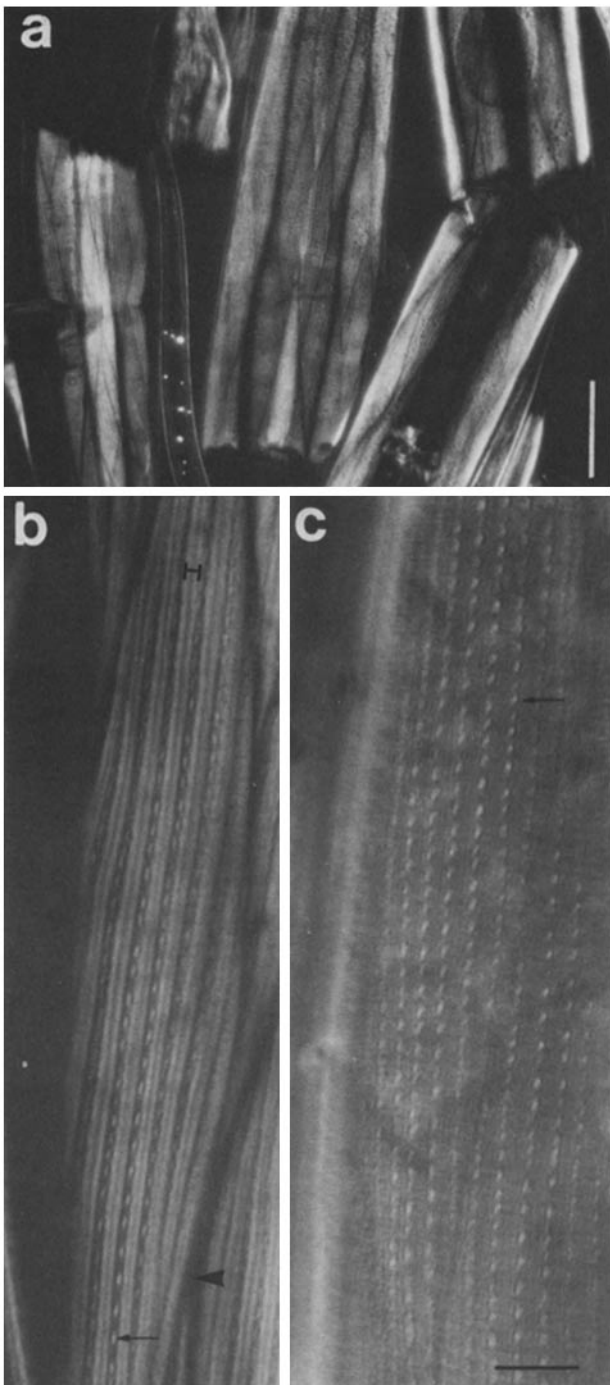
FIGURE 4 Micrographs of French-press sheared worm fragments extracted with 1% NP-40. Polarizing optics. (a) At low magnification (× 248), muscle birefringence can be seen to remain closely associated with cuticle, even at the broken ends of the fragments. Bar, 50 μm. (b) At higher magnification, muscle organization appears similar to that in undisrupted animals (Fig. 2c). Arrow, dense-body; arrowhead, muscle–muscle cell boundary; H, A-band. (c) Fragment extracted with 0.6 M NaCl/ATP buffer. A-band birefringence is virtually absent, but dense-bodies are still evident. (b and c) Bar, 5 μm. × 1,900.

clonal antibodies to uncharacterized nematode muscle proteins. Accordingly, we immunized mice with both NP-40/high-salt-extracted fragments and an extract of SDS-soluble proteins made from the same preparations (under nonreduc-

ing conditions to prevent solubilization of the sulfhydryl cross-linked cuticle proteins [10]). From hybridomas produced from one strongly responding mouse, we recovered ten cell lines that by immunofluorescent screening of supernatants were judged to secrete antibodies reactive with components of the I-band.

Antibody Localization in the Body Wall Musculature

On initial examination, these ten antibodies could be grouped into four classes based on their patterns of binding to the body wall musculature as viewed by fluorescence microscopy of specimens prepared by several methods (see Materials and Methods). Although the staining by three of the classes (defined by two class 1 and two class 2 antibodies, and one class 3 antibody) correlated with the spatial distribution of dense-bodies, the various classes could be distinguished by differences in the extent of their reaction with the dense-body and other elements of the muscle lattice. The fourth class, composed of five antibodies, stained the entire I-band except for the positions of dense-bodies.

The localization of the class 1 antibodies, MH35 and MH40, is shown in Figs. 5 and 6a, as viewed by direct immunofluorescence using monoclonal antibodies conjugated with TMRITC. In these tangential focal planes, staining by both antibodies was confined to intense spots of fluorescence aligned in rows oriented parallel to A–I bands. In detergent-extracted preparations (Fig. 5, b and c), the body wall musculature could be viewed with phase-contrast optics which revealed phase-dense A-bands interspersed with lighter I-bands, each containing a row of dark dense-bodies. The most intense spots of fluorescence corresponded to the location of dense-bodies viewed with phase optics. In radial optical sections that sampled the myofilament lattice approximately perpendicular to the cuticular surface, the class 1 antibodies appeared to stain the full extent of the dense-body though the depth of the lattice (Fig. 6a, inset). In both radial and tangential focal planes, the staining within the dense-body appeared homogeneous.

Despite strong staining of dense-bodies by the class 1 antibodies, their fluorescence was excluded from zones centered on those muscle–muscle cell boundaries that by electron microscopy were found to contain half I-bands with attachment plaques. As seen in Fig. 6a, these unstained zones corresponded, approximately, to the width of two sets of A–I bands, and extended across the muscle quadrant at a shallow angle to the longitudinal axis, and thus to the axes of myofilaments. This exclusion of staining from the cell margin regions corresponding to half I-bands demonstrates that the class 1 antibodies did not react with the attachment plaques in samples prepared by several different methods (e.g., Figs. 5a and 6a). A different pattern was observed in regions of the cell margin oriented approximately parallel to the myofilaments, at longitudinal muscle–muscle cell junctions as well as at the edges of the muscle quadrants. In these regions, the last dense-body in each I-band was situated near the cell boundary, and the rows of dense-bodies in adjacent cells often appeared to be aligned across cell boundaries.

The class 2 antibodies, MH23 and MH24, also reacted with the body wall musculature in a pattern that corresponded to the spatial distribution of dense-bodies. When compared directly in tangential focal planes, class 2 staining, represented
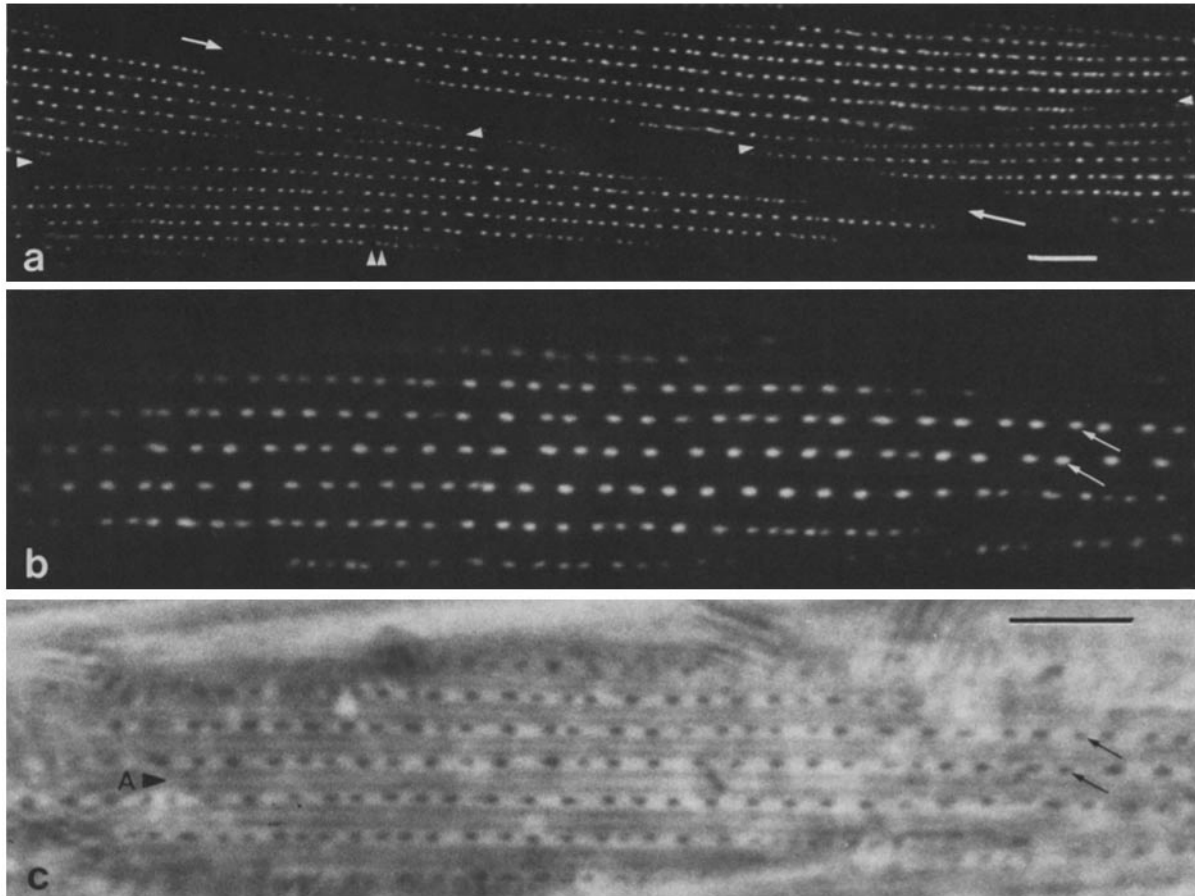
FIGURE 5 Fluorescence and phase micrographs of the body wall musculature stained with class 1 antibodies. (a) TMRITC-MH40 staining of several muscle cells in one quadrant of a subtilisin-digested animal. Symbols mark muscle–muscle cell boundaries oriented either obliquely (arrows), or approximately parallel (single arrowheads) to the animal's long axis. Bar, 5 μm. × 1,790. (b and c) Comparison of TMRITC-MH35 staining (b) in one muscle cell with the corresponding field viewed with phase optics (c). In c, A-bands (A) alternate with lighter I-bands containing dark dense-bodies (arrows). Fluorescence is coincident with the dense-bodies. The variable brightness of different dense-bodies appears to correlate with their phase-density. French-press sheared and NP-40-extracted worm fragment. Bar, 5 μm. × 3,125.

by FITC-MH23 in Fig. 6 b, was, for the most part, coincident with the fluorescence of class 1 antibodies. The two classes could be distinguished however by two criteria. The more easily perceived difference was the presence of class 2 staining along muscle–muscle cell boundaries, with strong fluorescence at oblique cell boundaries that contain half I-bands with attachment-plaques, and weak, variable staining along boundaries oriented parallel to the longitudinal axis. A second difference was observed in radial focal planes (Fig. 6, insets): whereas class 1 staining extended into the myofilament lattice area as already noted, the fluorescence of class 2 antibodies was confined to a narrow zone at or subjacent to the base of the dense-body, i.e., the region adjoining the plasmalemma and the overlying basement membrane. In samples observed by indirect immunofluorescence after reaction with both a class 1 and a class 2 antibody, no unstained gap could be detected separating the signal from each of the two antibodies (not shown).

A single monoclonal antibody, MH25, defined a third pattern of fluorescence. As with the class 2 antibodies, strong MH25 staining was present in regions that corresponded to the distribution of dense-bodies and the obliquely oriented cell margin regions containing attachment-plaques, and weak staining was observed inconsistently along longitudinal mus-

cle cell boundaries (Fig. 7 a). In addition, however, a discontinuous strip of fluorescence followed the center of each A-band. When viewed in radial focal planes, both the staining centered in the A-band and that associated with the dense-body was confined to a narrow zone closely apposed to the muscle cell surface (Fig. 7 b, inset). Thus, MH25 reacted with the base of the dense-body or an adjacent element near the plasma membrane similiarly to the class 2 antibodies, but in addition it also marked the base of the A-band in the region where the M-line is continuous with the plasma membrane. At high magnification (Fig. 7 b), the A-band-associated labeling appeared as an array of short staggered lines, perhaps reflecting the discontinuous but partially overlapping organization of the M-line densities observed by electron microscopy (Waterston, R. H., unpublished observation).

A fourth pattern of staining of the body wall muscles was observed with each of the five class 4 antibodies (MH29, MH39, MH44, MH45, and MH47). In samples fixed with formaldehyde, tracks of fluorescence extended across the cell parallel to the orientation of A–I striations (shown for MH44 and MH29 in Fig. 8). Using phase optics (Fig. 8 c), these tracks were found to encompass the full width of the I-band except for spots of reduced staining that corresponded to the positions of dense-bodies. Staining of the half I-bands along
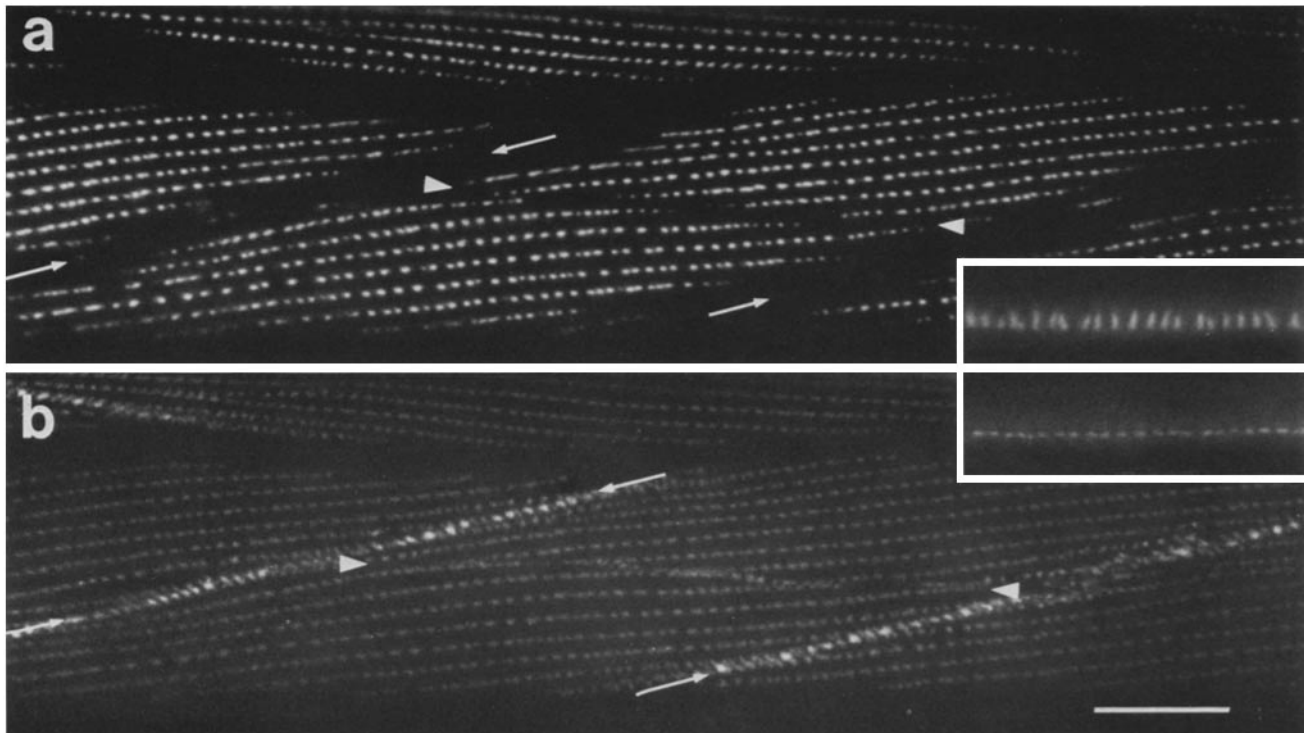
FIGURE 6   Direct immunofluorescence comparision of class 1 and class 2 antibody staining of NP-40–washed worm fragments. (a) TMRITC-MH35 (class 1) staining of four cells in one quadrant, and part of one cell in a second quadrant (top). Muscle–muscle cell junctions bordered by half I-bands correspond to the unstained zones (arrows) oriented at a shallow angle to the long body axis. At longitudinal muscle cell boundaries (arrowheads) and cell margins defining the edge of the muscle quadrant, dense-bodies are present closer to the cell margin. (Sarcomere organization in these regions is as depicted at the edges of the diagram in Fig. 2b). (Inset) MH35 staining in a radial optical section, approximately perpendicular to the cuticle surface. (b) FITC-MH23 staining of the same field as in a. In addition to fluorescence that corresponds to the positions of the dense-bodies, there is strong staining along the cell boundaries with half I-bands where class 1 staining is absent. (Inset) MH23 staining of the same field as in the inset in a; fluorescence is restricted to the base of each dense-body. Bar, 10 μm. × 1,730.
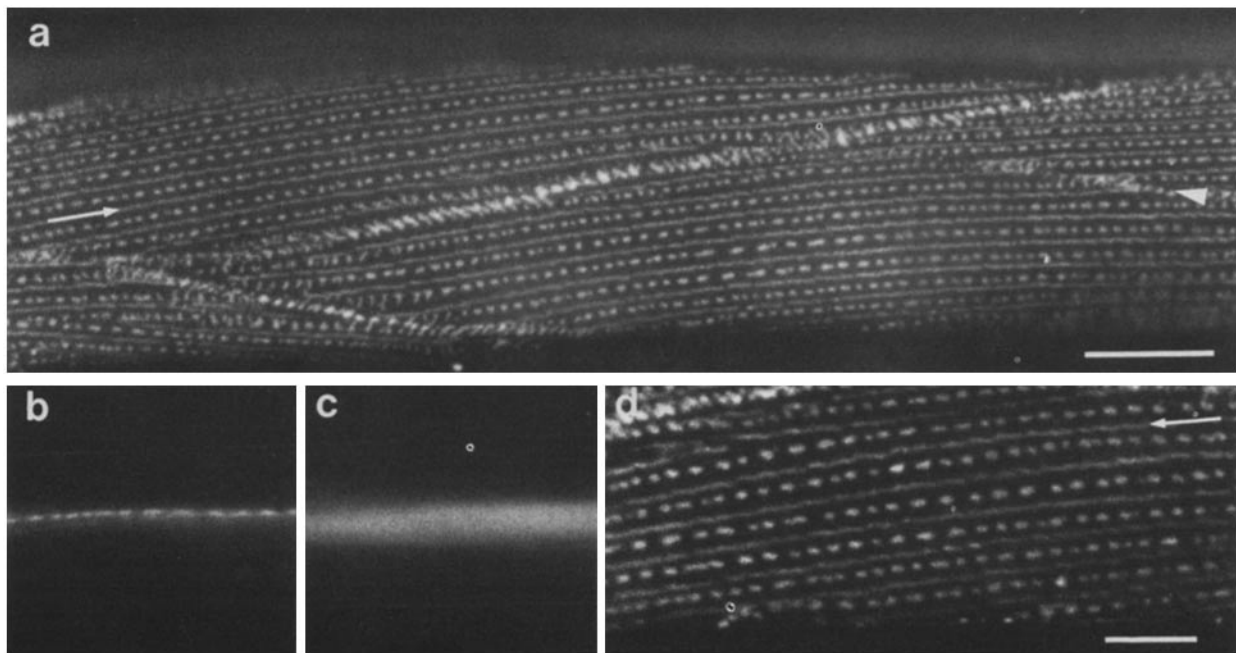

FIGURE 7   Fluorescence micrographs of the body wall musculature of NP-40–washed fragments stained with MH25. (a) Parts of four cells showing fluorescence corresponding to the positions of the dense-bodies, the center of each A-band (arrow), and cell boundaries (arrowhead). Bar, 10 μm. × 1,740. (b and c) Comparison of MH25 staining (b) in a radial optical section with the same field stained with fluorescein–phalloidin (c). MH25 fluorescence in b is confined to a narrow focal plane near the cell surface, peripheral to phalloidin staining of F-actin in c. × 1,740. (d) At high magnification, the MH25 fluorescence at the base of the A-band (arrow) is discontinuous, and often appears to consist of a series of partially overlapping but separate lines. Bar, 5 μm. × 2,450.
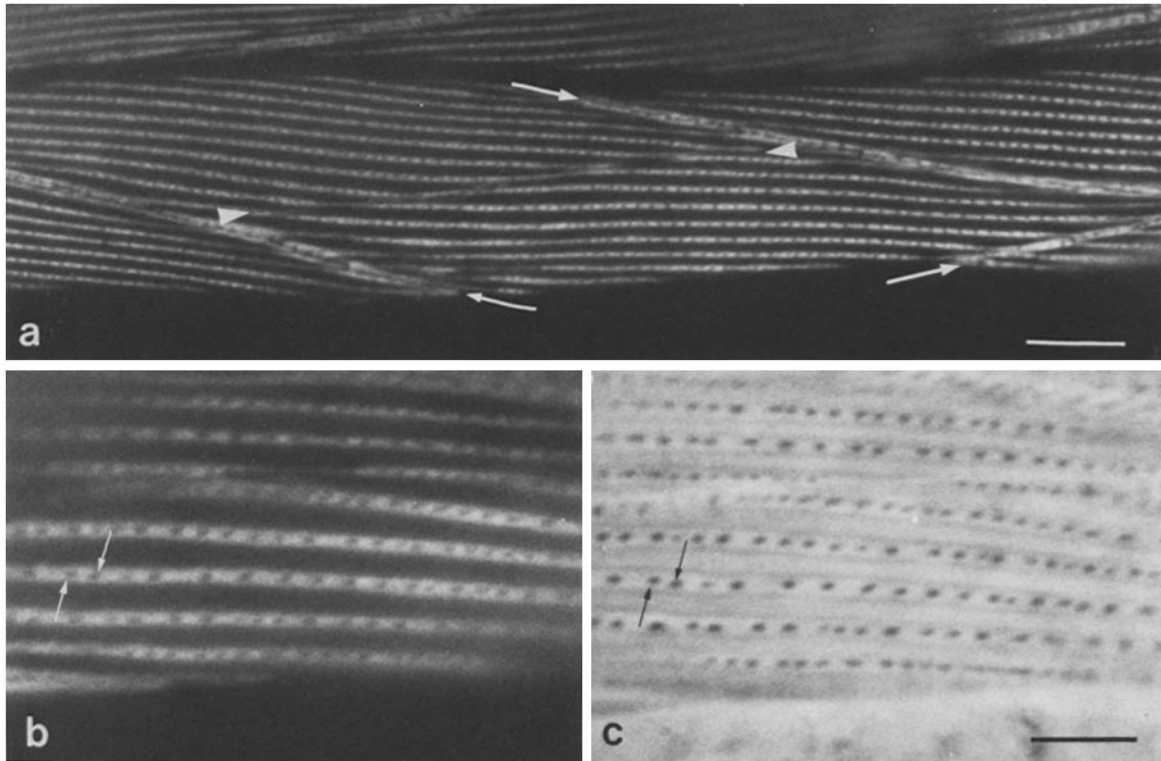
1540

FIGURE 8 Fluorescence micrographs of body wall musculature stained with the class 4 antibodies MH29 (a) and MH44 (b). (a) Tracks of fluorescence traverse the cell, ending at the edges of the muscle quadrant and along longitudinal muscle–muscle cell boundaries (arrowheads). Fluorescence near obliquely oriented cell boundaries bordered by half I-bands (arrows) appears as two irregular bands separated by an unstained gap. Bar, 10 μm. × 1,360. (b and c) Comparison of MH44 staining (b) with the corresponding field viewed with phase optics (c). Fluorescence encompasses the entire I-band except for the positions of dense-bodies which appear as unstained spots (arrows). Bar, 5 μm. × 2,850.

oblique muscle cell boundaries consistently appeared as two irregular but complementary bands in adjacent cells separated by an unstained gap (Fig. 8a, arrows). The width of the I-band staining was often variable within a single cell and between different cells. We have been unable to determine whether this variability resulted from muscle shortening as increased thick–thin filament overlap in obliquely striated muscle translates into a smaller decrease in I-band width than the corresponding changes in cross-striated muscle. Generally, however, the fluorescence was most narrow in those detergent-washed fragments in which the musculature appeared to be hypercontracted as judged by extensive folding of the overlying cuticle. This restriction of class 4 staining to the I-band cannot be accounted for by a general problem of antibody penetration of the A-band, because other monoclonal IgG antibodies have been found to stain the C. elegans A-band (39; and our unpublished observations). Class 4 antibody staining of unfixed worm fragments was similar to formaldehyde-fixed samples, but a different pattern was observed with each of the five antibodies after fixation in methanol or acid-alcohol (not shown). Because this pattern (which consisted of staining limited to very narrow regions between dense-bodies) differed from the continuous I-band fluorescence of unfixed and formaldehyde-fixed samples, it may arise from antigen loss or rearrangement during alcohol fixation.

Epitope Localization in a Single-Sarcomere Muscle

In addition to the body wall muscles, hermaphrodites con-

tain other specialized muscles involved in feeding, egg-laying, and defecation (2, 48). These small muscles differ from one another in their myofilament organization, but they generally contain the equivalent of a single sarcomere in which thin filaments attach to the cell membrane at opposite ends of the cell and interdigitate with a single set of bipolar thick filaments. Because the myofilament arrangement of several of these muscles, particularly the anal depressor muscle, resembles cross-striated muscle more closely than the body wall musculature, these muscles provide comparative information for interpreting antigen localization within the contractile lattice. As the findings of antibody staining in the anal depressor are, with few exceptions, representative of other single sarcomere muscles, only data for this muscle is presented.

The single anal depressor muscle cell is H-shaped, with each arm of the cell extending from the dorsal hypodermis to the ventrally placed rectum (49). Actin filament bundles, visualized with the F-actin binding phallotoxin, phalloidin (66), conjugated with fluorescein, attach at the end of each arm of the cell and extend toward the cell center (Fig. 9a). Of the four antibody classes, only the class 1 (anti-full dense-body) antibodies did not stain the anal muscle. Since this muscle effectively contains only half I-bands, this observation is consistent with the finding that the class 1 antibodies did not stain the half I-band attachment plaques in the body wall musculature. The class 1 antibodies did however react with other structures in the tail including apical cytoplasm of the intestinal epithelial cells (Fig. 9e) and the specific rectal cells that like the intestine are lined by microvilli (49). The class 2
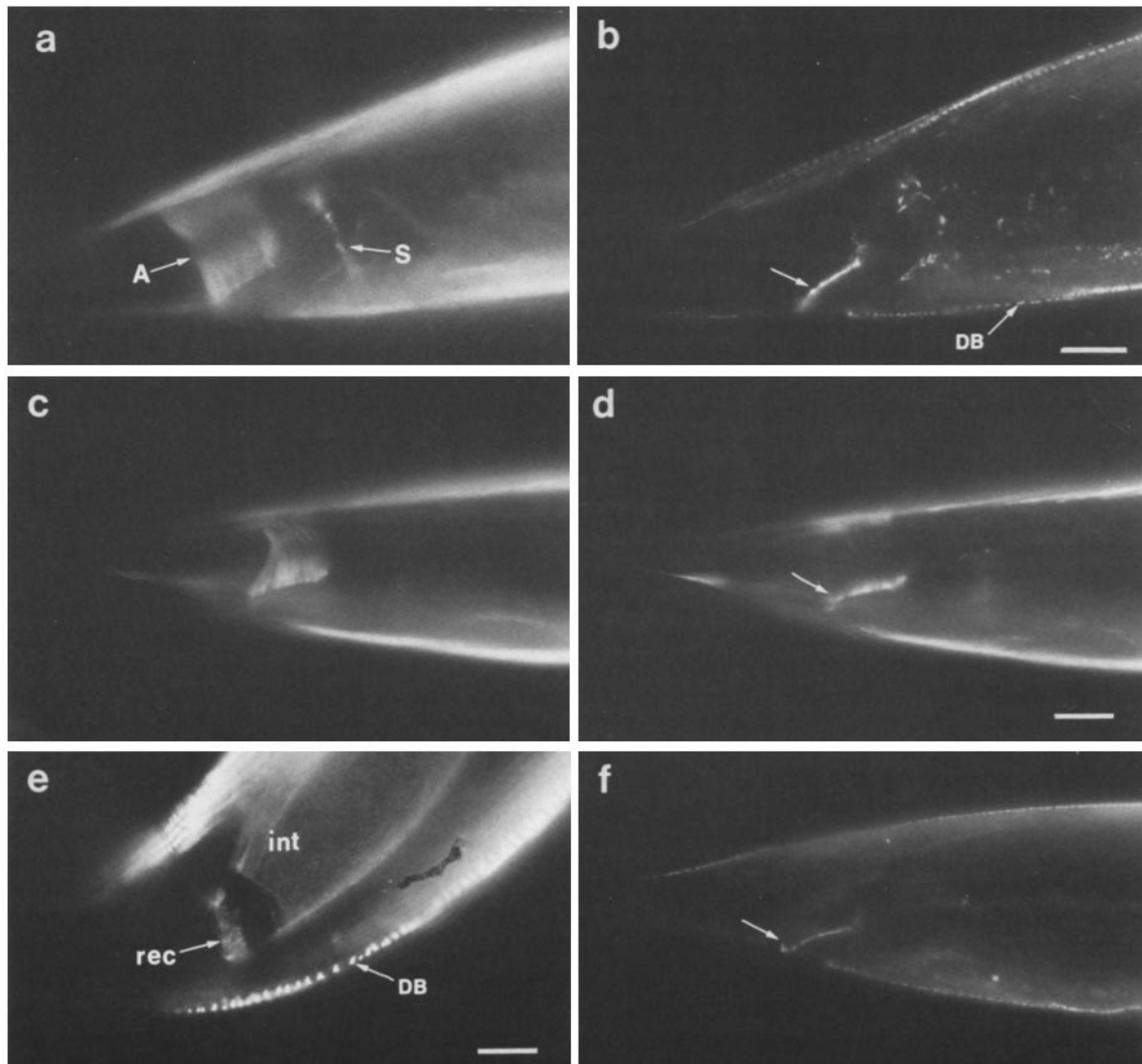
FIGURE 9 Fluorescence micrographs of the hermaphrodite tail stained with antibodies of each class. Right lateral views of NP-40–washed worm fragments, throughout, with anterior at right. (a) Fluorescein-phalloidin staining to visualize F-actin filament distribution in one arm of the anal depressor muscle (A) and in the sphincter muscle (S). The body wall musculature is detected as strong dorsal and ventral fluorescence (top and bottom). (b) Same field as in a stained with MH24 (class 2). The fluorescence associated with the anal muscle lies near the ventral cell surface (arrow) (similar staining is present at the dorsal surface which is below the plane of focus in this series). The sphincter muscle and the body wall muscle dense-bodies (DB) are also stained. × 860. (c and d) Paired micrographs comparing fluorescein-phalloidin (c) and MH44 (class 4) staining (d). MH44 fluorescence (arrow) coincides with the edge of phalloidin staining near the ventral surface of the anal muscle. × 760. (e) MH35 (class 1) staining. The anal muscle is unstained. Intestinal (int) and rectal (rec) epithelial cell that bear microvilli are stained but only in a narrow region of the apical cytoplasm. × 780. (f) MH25 (class 3) staining of the anal muscle, near the ventral cell surface (arrow). All bars, 10 μm. × 760.

antibodies (Fig. 9b) and MH25 (Fig. 9f) stained the anal muscle in a similar pattern. Their staining was limited to the ventral and dorsal cell surface regions where thin filaments originated, but could not be localized with respect to the cell membrane. The class 4 antibodies reacted near these same cell boundaries (Fig. 10d), but their fluorescence extended farther into the cell interior, partially overlapping with phalloidin staining. In summary, the localization of the various antigen classes in the anal depressor and other muscles examined paralleled their distribution in the body–wall musculature; class 1 staining was absent at sites where thin filaments end at the cell membrane, class 2 antibodies and MH25 reacted near membrane–thin filament attachment sites, and

class 4 antibodies stained part or all of the I-band equivalent of these muscles.

Polypeptide Specificities of Monoclonal Antibodies

The specificities of the four antibody classes were investigated by probing NC replicas of acrylamide/SDS gels with individual monoclonal antibodies, followed by a rabbit anti-mouse IgG and ^{125}I-protein A (52). Fig. 10 shows the protein fractions described in Fig. 1 analyzed on a Coomassie Blue-stained gel, and corresponding NC replicas probed with class 1 and class 2 antibodies. Both the class 1 antibodies, repre-
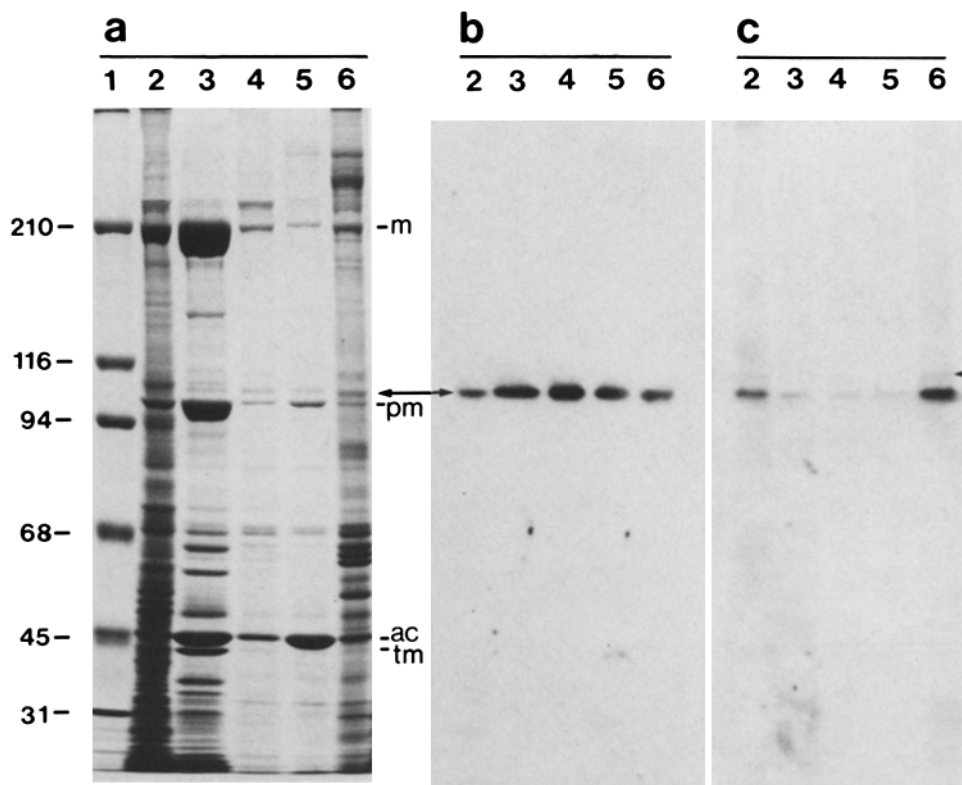
FIGURE 10 Identification of antigens recognized by class 1 and class 2 antibodies by Western transfer analysis. Protein fractions prepared as outlined in Fig. 1 were separated on 7.5% gels, and either stained with Coomassie Blue (a) or transferred to NC and probed with the class 1 antibody MH35 (b) or the class 2 antibody MH24 (c). (a) Coomassie Blue staining: lane 1, M_r standards × 10^{-3}; lane 2, total SDS-soluble nematode proteins; lane 3, actomyosin (0.6 M NaCl) extract; lane 4, 0.4% deoxycholate extract; lane 5, 0.5 M KSCN extract; lane 6, 8 M urea extract. Myosin heavy chain (m), paramyosin (pm), actin (ac), and tropomyosin (tm) are major components of the actomyosin extract. (b and c) Autoradiograms showing binding of MH35 (b) or MH24 (c). Both antibodies detect a 107,000 M_r band that aligns with a minor 107-kD polypeptide (arrow). In b, the antigen recognized by the class 1 antibody is most strongly represented in the 0.6 M NaCl, deoxycholate, and KSCN extracts, whereas in c, class 2 antibody binding is detected only in the lanes of total nematode proteins and the 8 M urea extract. The class 2 antibody also reacted weakly with a 110,000 M_r band (arrowhead).

sented by MH35 (Fig. 10b), and the class 2 antibodies, represented by MH24 (Fig. 10c), reacted with bands of ~107,000 D which were not resolved from one another. The antigen recognized by the class 1 antibodies was detected in all fractions, but was most strongly represented in the 0.4% deoxycholate fraction (lane 4) where it aligned with a minor Coomassie Blue–stained band. The antigen identified by the class 2 antibodies, in contrast, was detected only in the lanes containing total soluble nematode proteins (lane 1) or the 8 M urea extract (lane 6). In addition to this 107,000-D band, both class 2 antibodies also reacted weakly but consistently with a minor band of 110 kD, present in the same two samples.

The differences in the reactivity of class 1 and class 2 antibodies with the particular protein fractions led us to analyze the deoxycholate and 8 M urea fractions by two-dimensional gel electrophoresis (42). As shown in Fig. 11a, two-dimensional separation resolved the M_r 107,000 band into two sets of spots differing in isoelectric point. The more acidic of the two species, designated p107a, migrated as a single spot with an isoelectric pH of 6.1. The more basic species, p107b, consisted of several closely migrating isoelectric point variants centered at pH 6.6 (which were more easily distinguished on underloaded gels stained with silver [not shown]). When tested for binding to polypeptides in the 0.4%

deoxycholate fraction, the class 1 antibodies, MH35 (Fig. 11b) and MH40, reacted strongly with the acidic M_r 107,000 polypeptide, p107a. With the same fraction, the class 2 antibodies, MH24 (Fig. 11c) and MH23, in contrast, detected the basic M_r 107,000 species, p107b, and weakly identified the M_r 110,000 species, p110. A stronger signal with both class 2 antibodies was observed with the 8 M urea extract in which p107b and p110 were more abundant (Fig. 11d).

To determine if the different class 1 and class 2 antibodies recognized different epitopes of p107a and p107b/110, respectively, competition between antibodies for binding to antigen was examined using a qualitative direct immunofluorescence assay (see Materials and Methods for details). In control experiments, the signal from FITC-conjugated antibodies was diminished in samples that had been preincubated with an excess of the same unlabeled antibody as compared with samples preincubated with an irrelevant monoclonal IgG (not shown). With reciprocal combinations of the two different class 1 antibodies, one unlabeled and the other labeled with FITC, preincubation with the unlabeled antibody did not noticeably inhibit staining by the FITC-conjugate (i.e., staining was of similar intensity to that shown in Figs. 5 and 6). Similarly, neither class 2 antibody noticeably inhibited binding of the other. These results indicate that MH35 and MH40 recognized different determinants of p107a, and
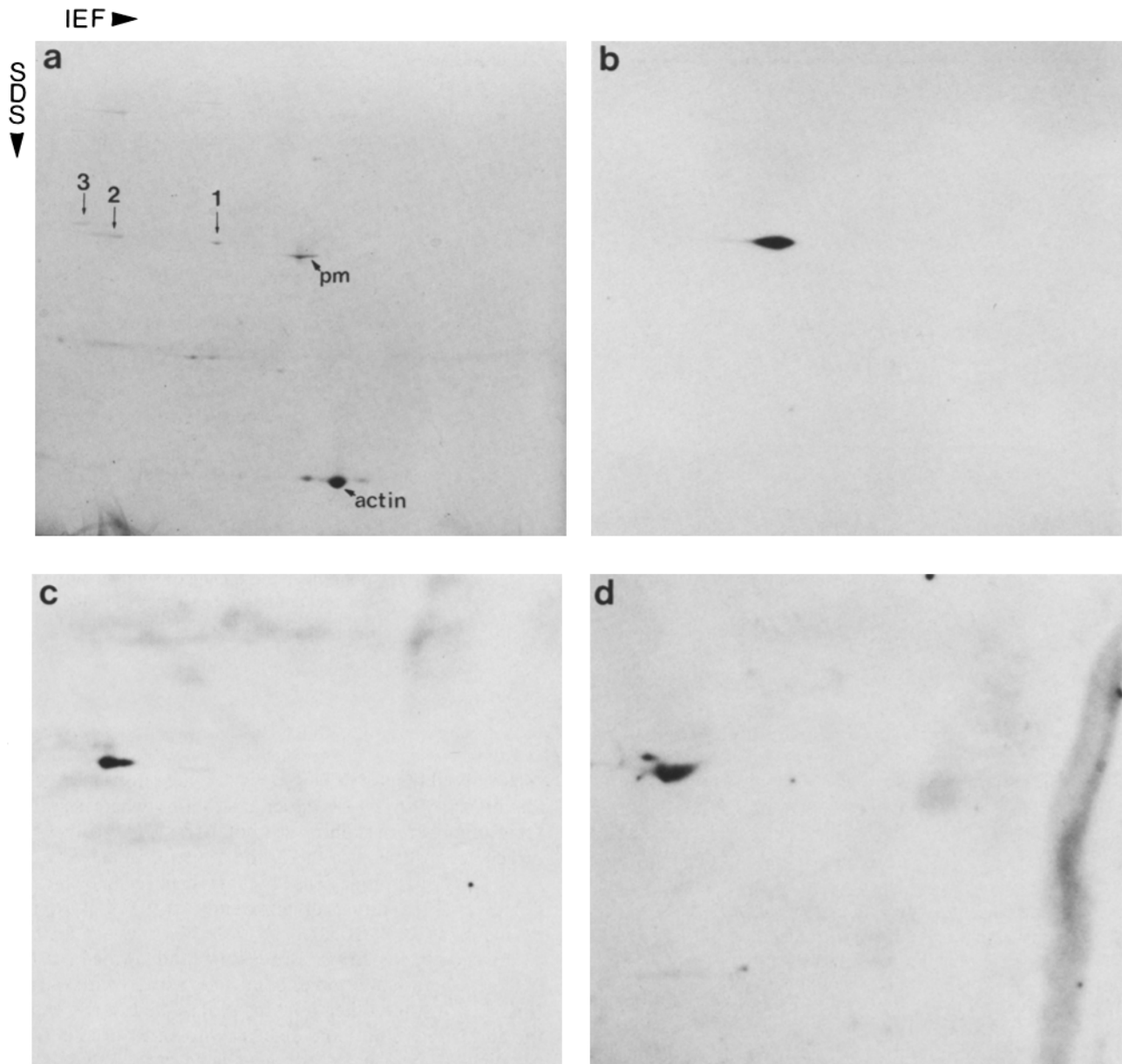
IEF ►

S
D
S
▼

FIGURE 11 Identification of class 1 and class 2 antigens among proteins separated by two-dimensional gel electrophoresis (42) and transferred to NC. (a) Coomassie Blue–stained two-dimensional gel (7.5% second dimension) containing a 1:1 mixture of 0.4% deoxycholate and 8 M urea extracts. The arrows mark the positions of p107a (1, pl 6.1), p107b (2, pl 6.6), or p110 (3), and pm indicates paramyosin. Isoelectric focusing, in gels containing 1.6% pH 5–7 and 0.4% pH 3.5–10 ampholytes, was for 15 h at 500 V and then 1 h at 800 V. (b and c) Autoradiograms of NC transfers of two-dimensional gels reacted with the class 1 antibody MH35 (b) or the class 2 antibody MH24 (c). Gels were run as in a, but were loaded with a 0.4% deoxycholate extract only. The immunoreactive spots were identified as p107a in a, or p107b in b, by comparison with the same filters stained with amido black (not shown). (d) Two-dimensional gel replica containing 8 M urea extract polypeptides only reacted with the class 2 antibody MH23. Both class 2 antibodies, represented here by MH23, bound to p110 in addition to p107b.

MH23 and MH24, different determinants of p107b/110.

Initial experiments examining the specificities of the class 4 antibodies indicated that each antibody bound to several very high molecular weight antigens. Protein extracts were thereafter run on 4% gels for greater resolution of large proteins (Fig. 12 a). Under these conditions, each of the class 4 antibodies (represented by MH39 and MH44 in Fig. 12) recognized a common set of high molecular weight components most strongly represented in the 0.5 M KSCN (lane 4) and 8 M urea (lane 5) extracts and the total nematode protein sample (lane 1). In the later fraction, two major bands were detected that migrated with mobilities corresponding to ap-

parent molecular weights of ~440,000 and 400,000, as roughly estimated using myosin heavy chain (M_r 210,000), filamin (M_r 250,000), and unreduced α2-macroglobulin (M_r 380,000) as standards. Both of these bands, which we designate p440/400, were also solubilized in 8 M urea (lane 5), but the trailing band was underrepresented in 0.5 M KSCN extracts (lane 4) in comparison with the leading band. In addition to p440/400, a lower molecular weight band was observed in the KSCN and urea extracts. This component and other minor bands were more prominent in samples prepared in the absence of protease inhibitors, suggesting they represent degradation products of p440/400 generated during sample
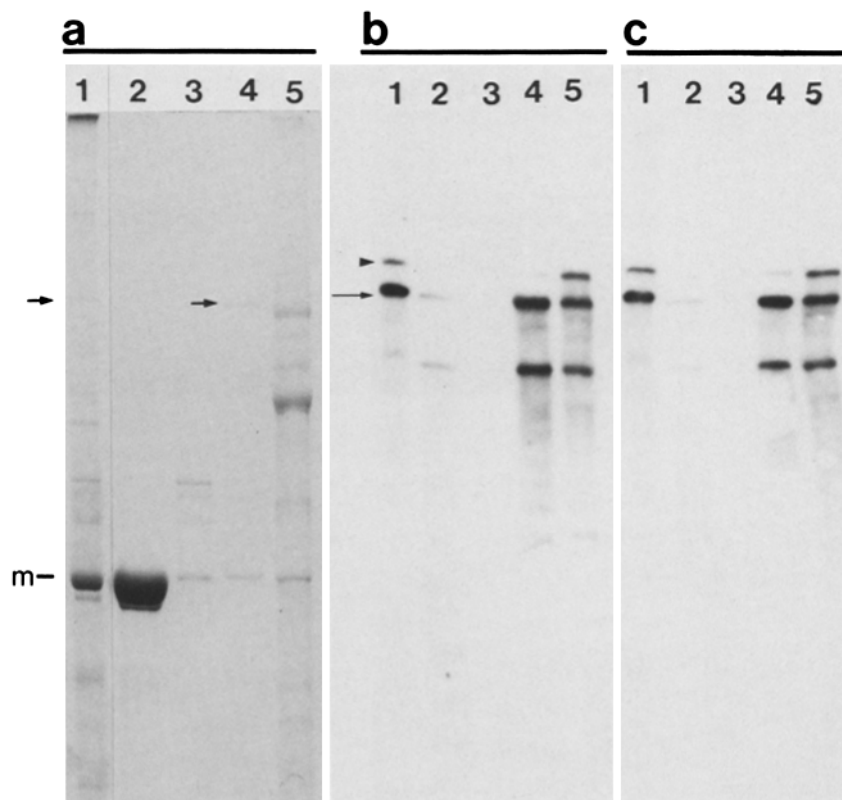
FIGURE 12 Determination of antigens recognized by class 4 antibodies. Nematode protein fractions were separated on 4% acrylamide/SDS gels and either stained with Coomassie Blue (a) or transferred to NC and probed with the class 4 antibodies MH39 (b) or MH44 (c). Lane 1, total SDS-soluble nematode proteins; lane 2, actomyosin extract; lane 3, 0.4% deoxycholate extract; lane 4, 0.5 M KSCN extract; and lane 5, 8 M urea extract. m, myosin heavy chain (M_r 210,000). (b and c) Autoradiographic detection of class 4 antibody binding. Each antibody detects two major bands, p400 (arrow in b) and p440 (arrowhead), and several lower molecular weight components. (The p400 band in lane 1 of b is skewed upward due to stretching of the gel in that region.) The reactive band p400 marked by an arrow in b corresponds to a minor polypeptide band on the stained gel (leftmost two arrows). A polypeptide corresponding to the trailing p440 band (arrowhead) was not detected by Coomassie Blue staining at the loadings used with this gel.

preparation. On comparison with the corresponding Coomassie Blue-stained gel (Fig. 12a), the two major reactive bands p440/400 aligned with minor components barely visible by protein staining at the gel loadings used. The leading band, p400, was poorly resolved from a slightly faster migrating and more abundant component which, in contrast to p400, was detected only among 8 M urea solubilized polypeptides.

Using the same protein fractions as for the identification of p440/400 and the two 107,000-D polypeptides, we could not identify a specific antigen recognized by MH25.

p107a Is Antigenically Related to Vertebrate Muscle α-Actinin

In addition to developing monoclonal antibodies to p107a and p107b/110, we raised a rabbit antiserum to a mixture of p107a and p107b purified by Sepharose-4B gel filtration and preparative SDS gel electrophoresis. The staining of the body wall musculature with this serum as viewed by indirect immunofluorescence was that expected for activity against both p107a and p107b/110: the shapes of the dense-bodies were easily perceived as with class 1 (p107a) antibodies, and fluorescence was present at cell margins where class 2 (p107b/110) but not p107a antibodies reacted (not shown). On NC transfers of two-dimensional gels containing deoxycholate and 8 M urea extract polypeptides, the serum reacted strongly with both p107a and p107b/110 (Fig. 13a), and also weakly recognized paramyosin, a likely contaminant in the immunogen. The several lower molecular weight spots in Fig. 13a are probably degradation fragments of p107a and p107b/110 as they have also been detected with p107a or p107b/110 specific monoclonal antibodies (not shown).

The p107/110 serum was examined for cross-reactivity with vertebrate muscle by indirect immunofluorescence of rabbit psoas myofibrils. As shown in Fig. 14, the serum reacted with the myofibrillar Z-line under conditions where significant preimmune serum staining was not detected (not shown). The principal constituent of the Z-line of vertebrate skeletal muscle and smooth muscle dense-bodies is believed to be α-actinin (22, 37, 45), a dimer of apparently identical polypeptide chains of 100,000–105,000 D (50). When tested for cross-reactivity with chicken gizzard extracts and purified α-actinin, p107/110 serum antibodies bound specifically with α-actinin (Fig. 15). Among other proteins represented in the extracts, the antibody did not bind detectably to either desmin (22) or filamin (20), which are also associated with skeletal muscle Z-discs, or to vinculin, a 130,000-D protein implicated in actin filament attachment to the cell membrane in muscle (18) and nonmuscle (8, 17, 18) cells.

The subset of p107/110 serum antibodies that recognized α-actinin determinants were characterized further by first purifying the cross-reactive antibodies by affinity to chicken gizzard α-actinin, and then testing the purified antibodies for reaction with comparable amounts of p107a and p107b separated by two-dimensional electrophoresis. As shown in Fig. 13b, the purified antibodies reacted strongly with p107a and with chicken α-actinin, which was run as a positive control at one end of the second dimension gel. No binding to p107b or p110 was detected even after longer film exposure. To confirm the presence of p107b/110, the same filter, without treatment to remove previously bound antibodies and ^{125}I-protein A, was probed with unfractionated p107/110 serum. Strong labeling of both p107b/110 and p107a was observed after a short exposure (Fig. 13c).

DISCUSSION

The attachment of C. elegans muscle to the cuticle by rela-

a IEF ——→

S D S ↓

b

c

↑ ↑ ↑ ↑ ↑ ↑
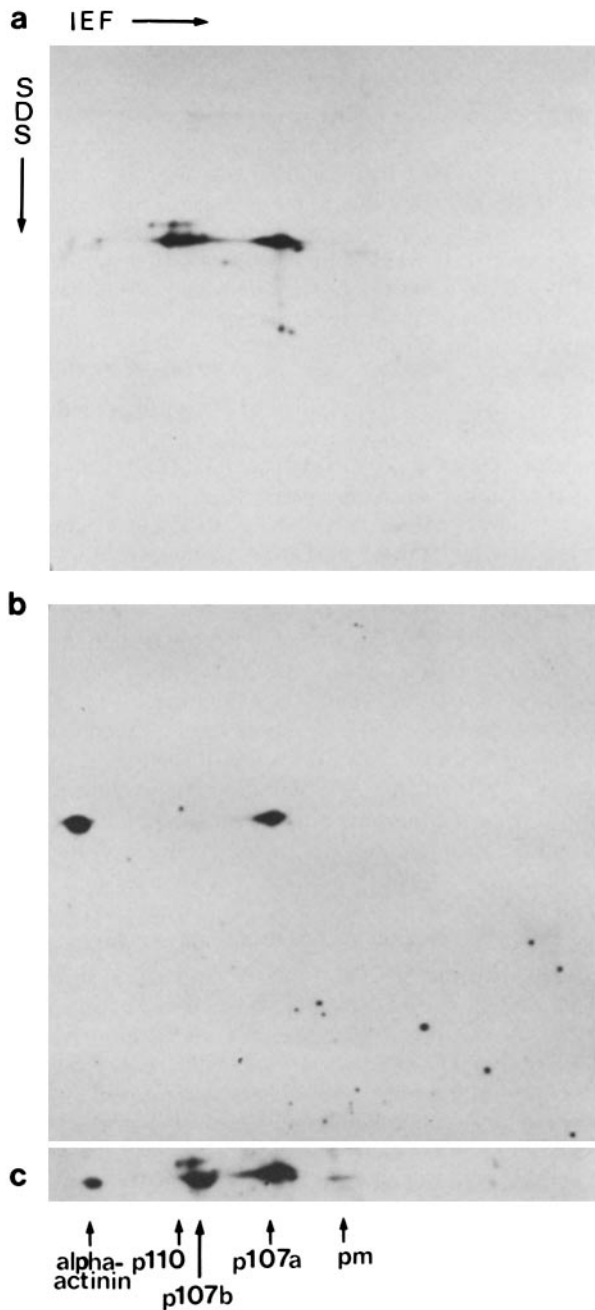alpha- p110 | p107a pm
actinin p107b

FIGURE 13 Analysis of the specificity of p107/110 serum antibodies. A 1:1 (vol/vol) mixture of 0.4% deoxycholate and 8 M urea extract polypeptides was run on two-dimensional gels and transferred to NC. (a) Binding of unfractionated antibodies detected by autoradiography. The major detected spots correspond from left to right to p110, p107b, p107a, and paramyosin (pm) (labeled at the bottom of the figure). Film exposure, 6 h. (b) Binding of cross-reactive p107/110 serum antibodies, purified by affinity to chicken gizzard α-actinin. In b, the sample and methods used were the same as in a except that purified chicken gizzard α-actinin was run at the far left of the second dimension gel. The purified antibodies bound only to α-actinin and p107a. Film exposure, 13 h. (c) Autoradiogram of the NC transfer shown in b after further treatment with unfractionated anti-p107/110 serum, followed by ^{125}I-protein A. Only the region containing isotopic labeling is shown. Film exposure, 3.5 h.

tively insoluble components has facilitated the identification, in this study, of several new proteins of obliquely striated muscle. These include two distinct 107,000 M_r proteins lo-
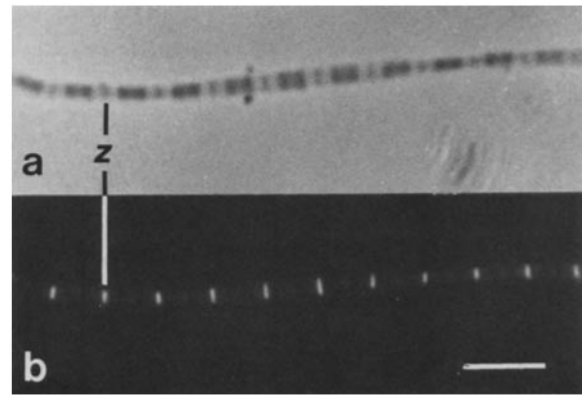

FIGURE 14 Cross-reactivity of p107/110 serum with a rabbit psoas muscle myofibril. Fluorescence in b aligns with the myofibril Z-line (z) seen with phase optics in a. Bar, 4.25 μm. × 2,350.
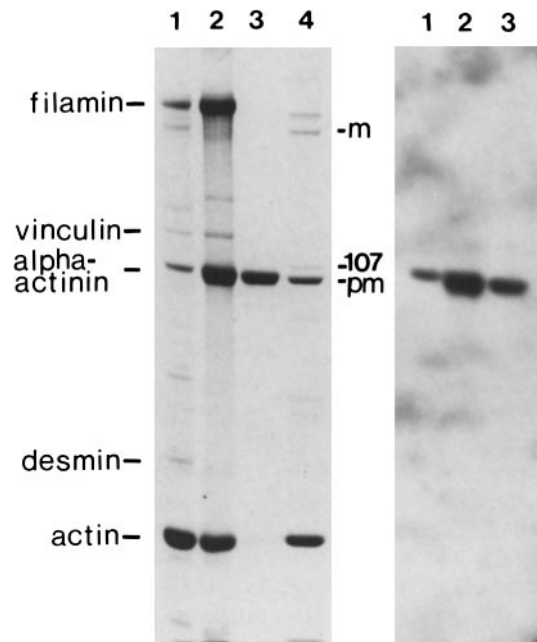

FIGURE 15 Cross-reactivity of p107/110 serum antibodies with chicken gizzard α-actinin. Left panel, 7.5% gel stained with Coomassie Blue. Lanes 1 and 2, chicken gizzard extracts; lane 3, purified chicken gizzard α-actinin; and lane 4, nematode 0.5 M KSCN extract. Chicken gizzard proteins are labeled at left, and nematode myosin heavy chain (m), M_r 107,000 proteins (107), and paramyosin (pm) are indicated at right. Right panel, autoradiogram of the corresponding NC transfer treated with p107/110 antibodies. Only α-actinin is detected among chicken gizzard proteins. Film exposure, 19 h.

calized to different domains of the dense-body, and a third antigen found closely apposed to the cell surface in regions overlying the dense-body and M-line analogue. Associated with the periphery of the dense-body and extending into the I-band is a fourth, high molecular weight component, not thought to be part of the thin filament.

At present, these assignments of antigen localization rest upon our interpretations of antibody staining as correlated with the organization of the body wall musculature observed in electron micrographs. A distinctive feature of the myofilament lattice is the apparent association of the dense body and M-line analogue with the cell membrane, and the persistent

association of both structures with the overlying basement membrane after partial extraction of other muscle components with nonionic detergent and 0.6 M NaCl. Although direct evidence is lacking, these observations, together with the distinctive morphology of the cell surface in regions overlying the dense-body and M-line (Fig. 3d), point to the existence of insoluble transmembrane components that mediate attachment of the dense-body and M-line to the basement membrane. The basement membrane in turn appears to be joined to the cuticle by hypodermal components which, as will be described elsewhere (manuscript in preparation), overlie the body wall muscles in a uniform pattern along the length of each muscle quadrant. The apparent attachment of the muscle lattice to hypodermal structures at frequent intervals suggests that muscle-generated tension is transmitted to the hypodermis and cuticle uniformly along the entire length of the cell. This property, coupled with other features of obliquely striated muscle (44), may enable individual contractile units to function independently but in sequence, and thereby facilitate the propagation of smooth contractile waves down the length of the animal.

The five class 4 monoclonal antibodies identify two high molecular weight polypeptides, designated p440/400, as constituents of the body wall muscle I-bands and the corresponding regions of other muscles examined. The relationship between these two polypeptides has not been determined, but in view of their susceptibility to degradation, the leading band could be a degradation product of the other, or both polypeptides might be derived from a larger, but as yet unidentified, component. The most significant properties of p440/400 determined here are its absence from the overlap zone of the A-band as shown by immunofluorescence localization, and its resistance to extraction with 0.6 M NaCl under conditions that solubilize known thin filament components including actin and tropomyosin. Both findings suggest that p440/400 comprises or is associated with an I-band structure other than the thin filament, but nonetheless do not rule out a potential function for these components in thin filament organization.

The p440/400 polypeptides may be related to one of several high molecular weight myofibrillar proteins that have been isolated from vertebrate skeletal muscle. Several large proteins have been characterized as likely components of intermediate filaments in vertebrate muscle and nonmuscle cells (5, 23, 65), for example, and the I-band distribution of p440/400 correlates with the location of intermediate-sized filaments in the body wall muscle cells of the larger nematode *Ascaris* (44). However, in the single sarcomere muscles in *C. elegans*, p440/400 is concentrated primarily near membrane–thin filament attachment sites, which is an unexpected distribution for intermediate filaments based on studies of vertebrate muscle and nonmuscle cells (30). Among other candidates for proteins analogous to p440/400 are two extremely large myofibrillar constituents, titin ($M_r \sim 1 \times 10^6$) and nebulin ($M_r \sim 10^5$), described by Wang et al. (56–58). Nebulin is located in the N2-line, a phase-dense region of the I-band, whereas titin has a more complex distribution, being detected at multiple sites in the sarcomere, but most prominently at the A–I junction. Although their functions are not known, it has been proposed that titin and nebulin comprise a filamentous and possibly elastic component of the sarcomere that corresponds to structures that have been observed in stretched and extracted muscle preparations (reviewed by Wang [56]). Perhaps

p440/400 forms part of an analogous structure in this invertebrate muscle.

A principal component of the dense body identified by the set of monoclonal antibodies studied here is a 107,000-D pI 6.1 polypeptide, designated p107a. In spite of the uniform staining of the dense body by p107a antibodies, the antigen could be concentrated in specific regions of the dense body such as the sites of thin filament attachment at the anterior and posterior ends. The similar sizes of p107a and chicken gizzard α-actinin and the finding that the two proteins share antigenic determinants suggest that p107a is a nematode α-actinin homolog. Further comparisons of p107a with α-actinin are required to test this view. In preliminary experiments, we have found that native p107a, purified with slight modifications of a method for α-actinin purification (13), parallels vertebrate α-actinin in its solubility and fractionation properties (unpublished observations).

Despite the apparent relatedness of p107a to α-actinin, its subcellular distribution differs from that expected for an α-actinin homolog in one significant aspect. In vertebrate muscle and nonmuscle cells, α-actinin has generally been implicated in thin filament attachment to the cell membrane by its association with specialized attachment structures such as smooth muscle attachment-plaques (18), the *fascia adherens* junction of cardiac muscle (53), and focal adhesion plaques in cultured fibroblasts (9, 31, 63). With nematode muscle, however, we find that p107a staining is not associated with the functionally analogous attachment plaques in the body wall muscle or with the corresponding regions of single sarcomere muscles where thin filaments in half I-bands terminate. Although loss or inaccessibility of the antigen cannot be ruled out as explanation for this result, our inability to detect staining at these sites using antibodies to two p107a epitopes and several preparation methods argues against this. We do not yet know whether a second protein analogous to p107a is present in these muscles or if p107a function is simply not required for thin filament attachment to the cell membrane. In the latter case, the nematode muscle attachment plaques would be analogous to certain sites in vertebrate cells (e.g., the tips of microvilli in the intestinal epithelium [7]) where thin filaments insert at the cell membrane, yet α-actinin is absent.

The class 2 antibodies identify a second constituent of the dense body comprising a 107,000-D, pI 6.6 polypeptide and a minor, slightly more basic 110,000-D species. In contrast to p107a, the p107b/110 polypeptides are confined to a narrow domain at or subjacent to the cell membrane, and are also present at the cell boundaries containing attachment plaques. In addition, p107b/110 is present in all single sarcomere muscles examined (Fig. 10 and unpublished observations) at sites consistent with its involvement in thin filament attachment in these muscles as well. At present, however, the position of p107b/110 with respect to the cell membrane is undetermined, which means that p107b/110 might function at any level in a sequence of components linking actin filaments to the cell surface. With the available immunological reagents, we have been unable to identify a vertebrate homolog of p107b, or to demonstrate relatedness between p107b and p107a. That the two proteins differ substantially is also indicated by their different extraction properties (Fig. 10) and by their different patterns of peptides generated by partial proteolysis (unpublished data). Despite the overall dissimilar-
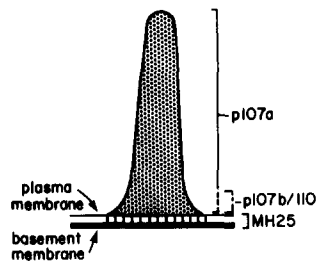
FIGURE 16 Model depicting the attachment of the dense-body to the plasmalemma and basement membrane, and the possible locations of p107a, p107b/110, and MH25 antigen. Broken lines indicate possible overlap in the distributions of p107a and p107b/110.

ity between their peptide patterns, we have also observed a few co-migrating p107a and p107b peptides that may perhaps represent conserved domains between functionally related proteins.

A third antigen, defined by the MH25 monoclonal antibody, is also found closely apposed to the cell membrane in regions of the dense-body and cell margin attachment plaque, but also at the center of the A-band where the M-line density joins with the plasmalemma. We have been unable to identify the antigen recognized by MH25, but its presence near the attachment sites of seemingly unrelated structures such as the dense-body and M-line can be explained most simply by the hypothesis that the antigen is a membrane or cell surface component. That the composition of the cell surface is specialized in these regions is indicated by its distinctive morphology, and also by the finding that the lectin concanavalin A stains the body wall musculature similarly to MH25 (our unpublished data). Two monoclonal antibodies that are indistinguishable from MH25 by histochemical criteria have been isolated by J. Lewis (personal communication). Since these antibodies were generated to nematode components fractionated in part by affinity to concanavalin A, they may recognize a glycoconjugate, presumably a membrane or cell surface molecule. Regardless, concanavalin A identifies a dense-body associated component other than p107b/110 which has no associated carbohydrate that we can detect by assays for lectin binding or periodate-sensitive hydroxyl groups.

The differences in the distributions of p107a, p107b/110, and the MH25 antigen detected with specific antibodies can be incorporated into the following model for their organization in the dense-body (Fig. 16). Reflecting the hypothesis that antigens associated with both the dense-body and M-line identify cell surface or membrane components, MH25 defines an attachment component associated with the basement membrane and/or the plasmalemma. p107b/110 and p107a define two cytoplasmic domains of the dense-body, with p107b/110 forming the membrane-proximal portion and p107a extending through the remainder of the dense-body and possibly into the p107b/110 domain. The uncertain positions of p107b/110 and the MH25 antigen with respect to the cell membrane make these assignments tentative, and the specific protein interactions that might determine such an organization are entirely unknown. The differential location of these components, however, is consistent with a sequential pathway of protein assembly that might be initiated on the cell membrane, perhaps at sites determined in part through interactions with the hypodermis. This process must occur not only in embryogenesis when muscle is first formed, but also as the body wall musculature grows during larval development. If dense-bodies are formed primarily at muscle–muscle cell junctions, the cell margin attachment plaques might then be utilized as an assembly intermediate from

which dense-bodies would be formed by the addition of p107a and other components.

The collection of monoclonal antibodies described here should prove useful as probes for examining the abnormalities in specific mutants with defective muscle structure. Additionally, the antibodies might be used to isolate the DNA sequences encoding the proteins from genomic or cDNA expression libraries (67). The structural gene encoding that product could, in turn, be mapped in the genome by in situ hybridization to nematode chromosomes as described by Albertson (1), or more precisely by genetic mapping of associated DNA polymorphisms as described for the C. elegans actin gene cluster (14). Mutations in the structural gene for that muscle product might then be identified by a detailed examination of mutants that map to the same region for molecular alterations associated with that gene.

REFERENCES

1. Albertson, D. G. 1984. Localization of the ribosomal genes in Caenorhabditis elegans chromosomes by in situ hybridization using biotin-labeled probes. EMBO (Eur. Mol. Biol. Organ.) J. 3:1227–1234.
2. Albertson, D. G., and J. N. Thomson. 1976. The pharynx of Caenorhabditis elegans. Philos. Trans. R. Soc. Lond. B. Biol. Sci. 275:299–325.
3. Batteiger, B., W. J. Newhall, and R. R. Jones. 1982. Use of Tween 20 as a blocking agent in the immunological detection of proteins transferred to nitrocellulose membranes. J. Immunol. Methods. 55:297–307.
4. Blose, S. H., D. I. Meltzer, and J. R. Feramisco. 1984. 10-nm Filaments are induced to collapse in living cells microinjected with monoclonal and polyclonal antibodies against tubulin. J. Cell Biol. 98:847–858.
5. Breckler, J., and E. Lazarides. 1982. Isolation of a new high molecular weight protein associated with desmin and vimentin filaments from avian embryonic skeletal muscle. J. Cell Biol. 92:795–806.
6. Brenner, S. 1974. The genetics of Caenorhabditis elegans. Genetics. 77:71–94.
7. Bretscher, A., and K. Weber. 1978. Localization of actin and microfilament-associated proteins in the microvilli and terminal web of the intestinal brush border by immunofluorescence microscopy. J. Cell Biol. 79:839–845.
8. Burridge, K., and J. R. Feramisco. 1980. Microinjection and localization of a 130K protein in living fibroblasts: a relationship to actin and fibronectin. Cell. 19:587–595.
9. Chen, W.-T., and S. J. Singer. 1982. Immunoelectron microscopic studies of the sites of cell-substratum and cell-cell contacts in cultured fibroblasts. J. Cell Biol. 95:205–222.
10. Cox, G. N., M. Kusch, and R. S. Edgar. 1981. Cuticle of Caenorhabditis elegans: its isolation and partial characterization. J. Cell Biol. 90:7–17.
11. Craig, R., and G. Offer. 1976. The location of C-protein in rabbit skeletal muscle. Proc. R. Soc. Lond. B. Biol. Sci. 192:451–461.
12. Epstein, H. F., and J. N. Thomson. 1974. Temperature sensitive mutation affecting myofilament lattice assembly in Caenorhabditis elegans. Nature (Lond.). 250:579–580.
13. Feramisco, J. R., and K. Burridge. 1980. A rapid purification of α-actinin, filamin, and a 130,000-dalton protein from smooth muscle. J. Biol. Chem. 255:1194–1199.
14. Files, J. G., S. Carr, and D. Hirsh. 1983. Actin gene family of Caenorhabditis elegans. J. Mol. Biol. 164:355–375.
15. Galfre, G., and C. Milstein. 1981. Preparation of monoclonal antibodies: strategies and procedures. Methods Enzymol. 73:3–46.
16. Galfre, G., S. C. Howe, C. Milstein, G. W. Butcher, and J. C. Howard. 1977. Antibodies to major histocompatibility antigens produced by hybrid cell lines. Nature (Lond.). 266:550–552.
17. Geiger, B. 1979. A 130K protein from chicken gizzard: its localization at the termini of microfilament bundles in cultured cells. Cell. 18:193–205.
18. Geiger, B., A. H. Dutton, T. T. Tokuyasu, and S. J. Singer. 1981. Immunoelectron microscope studies of membrane-microfilament interactions: distributions of α-actinin, tropomyosin, and vinculin in intestinal epithelial brush border and chicken gizzard smooth muscle cells. J. Cell Biol. 91:614–628.
19. Goldman, M. 1968. Fluorescent Antibody Methods. Academic Press, Inc., New York. 102–106.
20. Gomer, R. H., and E. Lazarides. 1983. Highly homologous filamin polypeptides have different distributions in avian slow and fast muscle fibers. J. Cell Biol. 97:818–823.
21. Gossett, L. A., R. M. Hecht, and H. F. Epstein. 1982. Muscle differentiation in normal and cleavage-arrested mutant embryos of Caenorhabditis elegans. Cell. 30:193–204.
22. Granger, B. L., and E. Lazarides. 1978. The existence of an insoluble Z-disc scaffold in chicken skeletal muscle. Cell. 15:1253–1268.
23. Granger, B. L., and E. Lazarides. 1980. Synemin: a new high molecular weight protein associated with desmin and vimentin filaments in muscle. Cell. 22:727–738.

24. Harris, H. E., M.-Y. Tso, and H. F. Epstein. 1977. Actin and myosin-linked calcium regulation in the nematode *Caenorhabditis elegans*. Biochemical and structural properties of native filaments and purified proteins. *Biochemistry.* 16:859–865.

25. Harris, H. E., and H. F. Epstein. 1977. Myosin and paramyosin of *Caenorhabditis elegans*: biochemical and structural properties of wild-type and mutant proteins. *Cell.* 10:709–719.

26. Hirumi, H., D. J. Raski, and N. O. Jones. 1971. Primitive muscle cells of nematodes: morphological aspects of platymyarian and shallow coelomyarian muscles in two plant parasitic nematodes, *Trichordorus christei* and *Longidorus elongatus*. *J. Ultrastruct. Res.* 34:517–543.

27. Knight, P. J., and J. A. Trinick. 1982. Preparation of myofibrils. *Methods Enzymol.* 85:9–12.

28. Krohne, G., R. Stick, J.A. Kleinschmidt, R. Moll, W. Franke, and P. Hausen. 1982. Immunological localization of a major karyoskeletal protein in nucleoli of oocytes and somatic cell of *Xenopus laevis*. *J. Cell Biol.* 94:749–754.

29. Landel, C. P., M. Krause, R. H. Waterston, and D. Hirsh. 1984. DNA rearrangements of the actin gene cluster in *C. elegans* accompany reversion of three muscle mutants. *J. Mol. Biol.* 180:497–513.

30. Lazarides, E. 1982. Intermediate filaments: a chemically heterogeneous, developmentally regulated class of proteins. *Annu. Rev. Biochem.* 51:219–250.

31. Lazarides, E., and K. Burridge. 1975. α-Actinin: immunofluorescent localization of a muscle structural protein in nonmuscle cells. *Cell.* 6:289–298.

32. Laemmli, U. K. 1970. Cleavage of structural proteins during the assembly of the head of the bacteriophage T4. *Nature (Lond.).* 227:680–685.

33. Mackenzie, J. M., R. L. Garcea, J. M. Zengel, and H. F. Epstein. 1978. Muscle development in *Caenorhabditis elegans*: mutants exhibiting retarded sarcomere construction. *Cell.* 15:751–762.

34. Mackenzie, J. M., F. Schachat, and H. F. Epstein. 1978. Immunocytochemical localization of two myosins within the same muscle cells in *Caenorhabditis elegans*. *Cell.* 15:413–419.

35. Mackenzie, J. M., and H. F. Epstein. 1980. Paramyosin is necessary for determination of nematode thick filament length in vivo. *Cell.* 22:747–755.

36. MacLeod, A. R., R. H. Waterston, R. M. Fishpool, and S. Brenner. 1977. Identification of the structural gene for a myosin heavy chain in *Caenorhabditis elegans*. *J. Mol. Biol.* 114:133–140.

37. Masaki, T., M. Endo, and S. Ebashi. 1967. Localization of 6S component of α-actinin at Z-band. *J. Biochem.* 62:630–632.

38. McLachlan, A. D., and J. Karn. 1982. Periodic charge distributions in the myosin rod amino acid sequence match cross-bridge spacings in muscle. *Nature (Lond.).* 299:226–231.

39. Miller, D. M., I. Ortiz, G. C. Berliner, and H. F. Epstein. 1983. Differential localization of two myosins within nematode thick filaments. *Cell.* 34:477–490.

40. Moerman, D. G., S. Plurad, R. H. Waterston, and D. L. Baille. 1982. Mutations in the *unc*-54 myosin heavy chain gene of *Caenorhabditis elegans* that alter contractility but not muscle structure. *Cell.* 29:773–781.

41. Moerman, D. G., and D. L. Baille. 1981. Formaldehyde mutagenesis in the nematode *Caenorhabditis elegans*. *Mutat. Res.* 80:273–279.

42. O'Farrell, P. H. 1975. High resolution two-dimensional electrophoresis of proteins. *J. Biol. Chem.* 250:4007–4021.

43. Rosenbluth, J. 1965. Structural organization of obliquely striated muscle fibers in *Ascaris lumbricoides*. *J. Cell Biol.* 25:495–515.

44. Rosenbluth, J. 1967. Obliquely striated muscle. III. Contraction mechanism of *Ascaris* body muscle. *J. Cell Biol.* 34:15–33.

45. Schollmeyer, J. E., L. T. Furcht, D. E. Goll, R. M. Robson, and M. H. Stromer. 1976. Localization of contractile proteins in smooth muscle cells and in normal and transformed fibroblasts. *In* Cell Motility. Book A. R. Goldman, T. Pollard, and J. Rosenbaum, editors. Cold Spring Harbor Laboratory, Cold Spring Harbor, NY. 361–388.

46. Schulman, M., C. D. Wilde, and G. Kohler. 1978. A better cell line for making hybridomas secreting specific antibodies. *Nature (Lond.).* 276:269–270.

47. Sulston, J. E., and S. Brenner. 1974. The DNA of *Caenorhabditis elegans*. *Genetics.* 77:95–104.

48. Sulston, J. E., and H. R. Horvitz. 1977. Post-embryonic cell lineages of the nematode *Caenorhabditis elegans*. *Dev. Biol.* 56:110–156.

49. Sulston, J. E., E. Schierenberg, J. G. White, and J. N. Thomson. 1983. The embryonic cell lineage of the nematode *Caenorhabditis elegans*. *Dev. Biol.* 100:64–119.

50. Suzuki, A., D. E. Goll, I. Singh, R. E. Allen, R. M. Robson, and M. H. Stromer. 1976. Some properties of purified skeletal muscle α-actinin. *J. Biol. Chem.* 251:6860–6870.

51. Takacs, B. J., and T. Staehelin. 1981. Biochemical characterization of cell surface antigens using monoclonal antibodies. *In* Immunological Methods. Volume II. I. Lefkovits and B. Pernis, editors. Academic Press, Inc., New York. 27–56.

52. Towbin, H., T. Staehelin, and J. Gordon. 1979. Electrophoretic transfer of proteins from polyacrylamide gels to nitrocellulose sheets: procedure and some applications. *Proc. Natl. Acad. Sci. USA.* 76:4350–4354.

53. Tokuyasu, K. T., A. H. Dutton, B. Geiger, and S. J. Singer. 1981. Ultrastructure of chicken cardiac muscle as studied by double immunolabeling in electron microscopy. *Proc. Natl. Acad. Sci. USA.* 78:7619–7623.

54. Trinick, J., and S. Lowey. 1977. M-protein from chicken pectoralis muscle: isolation and characterization. *J. Mol. Biol.* 113:343–368.

55. Wallimann, T., D. C. Turner, and H. M. Eppenberger. 1977. Localization of creatine kinase isozymes in myofibrils. I. Chicken skeletal muscle. *J. Cell Biol.* 75:297–317.

56. Wang, K. 1984. Cytoskeletal matrix in striated muscle: the role of titin, nebulin, and intermediate filaments. *In* Contractile Mechanisms in Muscle. G. H. Pollack, editor. Plenum Publishing Corp., New York. 285–305.

57. Wang, K., J. McClure, and A. Tu. 1979. Titin: major myofibrillar components of striated muscle. *Proc. Natl. Acad. Sci. USA.* 76:3698–3702.

58. Wang, K., and C. L. Williamson. 1980. Identification of an N2 line protein of striated muscle. *Proc. Natl. Acad. Sci. USA.* 77:3254–3258.

59. Waterston, R. H., R. M. Fishpool, and S. Brenner. 1977. Mutants affecting paramyosin in *Caenorhabditis elegans*. *J. Mol. Biol.* 117:679–697.

60. Waterston, R. H., J. N. Thomson, and S. Brenner. 1980. Mutants with altered muscle structure in *Caenorhabditis elegans*. *Dev. Biol.* 77:271–302.

61. Waterston, R. H., D. Hirsh, and T. R. Lane. 1984. Dominant mutations affecting muscle structure in *Caenorhabditis elegans* that map near the actin gene cluster. *J. Mol. Biol.* 180:473–496.

62. Weber, K., and M. Osborn. 1975. Proteins and sodium dodecyl sulfate: molecular weight determination on polyacrylamide gels and related procedures. *In* The Proteins. Volume 1. H. Neurath, R. L. Hill, and C.-L. Boeder, editors. Academic Press, Inc., New York. 179–223.

63. Wehland, T., M. Osborne, and K. Weber. 1979. Cell-to-substratum contacts in living cells: a direct correlation between interference-reflexion and indirect-immunofluorescence microscopy using antibodies against actin and α-actinin. *J. Cell Sci.* 37:257–273.

64. White, J. G., E. Southgate, J. N. Thomson, and S. Brenner. 1976. The structure of the ventral nerve cord of *Caenorhabditis elegans*. *Philos. Trans. R. Soc. London B. Biol. Sci.* 275:327–348.

65. Wiche, G., H. Herrmann, F. Leichtfried, and R. Pytela. 1982. Plectin: a high-molecular-weight cytoskeletal polypeptide component that copurifies with intermediate filaments of the vimentin type. *Cold Spring Harbor Symp. Quant. Biol.* 46:475–482.

66. Wulf, E., A. Deboben, F. A. Bautz, H. Faulstich, and Th. Wieland. 1979. Fluorescent phallotoxin, a tool for the visualization of cellular actin. *Proc. Natl. Acad. Sci. USA.* 76:4498–4502.

67. Young, R. A., and R. W. Davis. 1983. Efficient isolation of genes using antibody probes. *Proc. Natl. Acad. Sci. USA.* 80:1194–1198.

68. Zengel, J. M., and H. F. Epstein. 1980. Identification of genetic elements associated with muscle structure in the nematode *Caenorhabditis elegans*. *Cell Motil.* 1:73–97.

69. Zengel, J. M., and H. F. Epstein. 1980. Muscle development in *Caenorhabditis elegans*: a molecular-genetic approach. *In* Nematodes as Biological Models. Volume 1. B. M. Zuckerman, editor. Academic Press, Inc., New York. 73–126.